



<b>Publication Year</b>	2009
<b>Acceptance in OA @INAF</b>	2024-01-23T16:48:42Z
<b>Title</b>	GNSS Reconfigurable Antenna Based Enhanced Localization - WP1: GRABEL System specification and architecture - D1.4: Architecture and system specification
<b>Authors</b>	Consoli, Angelo; Lehmann, Christoph; Iera, Christian; Petit, Laurent; Ayadi, Jaouhar; et al.
<b>Handle</b>	<a href="http://hdl.handle.net/20.500.12386/34599">http://hdl.handle.net/20.500.12386/34599</a>
<b>Number</b>	WP1 - D1.4



**Project Number:** FP7 GRABEL\_232016  
{REF RTD REG/T.4(2008)D/566378}  
**Project Title:** GNSS Reconfigurable Antenna Based  
Enhanced Localization  
**Deliverable Type (Pub/Int)\*:** Pub

## GNSS Reconfigurable Antenna Based Enhanced Localization

FP7 GRABEL\_232016 {REF RTD REG/T.4(2008)D/566378}



### WP1: GRABEL System specification and architecture

#### D1.4: Architecture and system specification

**Contractual Date of Delivery to the CEC:** 30/09/2009

**Actual Date of Delivery to the CEC:** 30/09/2009

**Author(s):** Angelo Consoli<sup>1</sup> (editor), Christoph Lehmann<sup>1</sup>, Christian Iera<sup>1</sup>, Laurent Petit<sup>2</sup>, Jaouhar Ayadi<sup>2</sup>, Nicolae Chiurtu<sup>2</sup>, Francesco Piazza<sup>3</sup>, Roberto Materni<sup>3</sup>, Edgardo Arcuri<sup>3</sup>, Giovanni Naldi<sup>4</sup>, Baptiste Godefroy<sup>5</sup>, Jean-Baptiste Prost<sup>5</sup>, Ilias Andrikopoulos<sup>6</sup>, Dimitris Drandakis<sup>7</sup>, Christos Anagnostopoulos<sup>5</sup>,

**Participant(s):** <sup>1</sup>EXYS, <sup>2</sup>CSEM, <sup>3</sup>SYN, <sup>4</sup>INAF, <sup>5</sup>PSTAR, <sup>6</sup>SPH, <sup>7</sup>MOB

**Workpackage:** WP1 GRABEL System specification and architecture

**Est. person months:** 7 (1<sup>1</sup>, 1<sup>2</sup>, 1<sup>3</sup>, 1<sup>4</sup>, 1<sup>5</sup>, 1<sup>6</sup>, 1<sup>7</sup>)

**Nature:** R (Nature: P-prototype, R-report, O-other)

**Dissemination:** Pub (Type: Pub-public, Int-internal)

**Version:** 1.17

**Total number of pages:** 58

#### Abstract:

This deliverable is basically a high level specification of the GRABEL receiver and should serve as the guideline during its development. The two proposed applications are specified, and the requirements that need to be fulfilled by the GRABEL receiver to be successful in these 2 applications are listed. The structure and characteristics of the receiver are then described, where possible already in a quantitative manner. Particular attention was reserved to the antenna array. Given the relatively large dimensions that a beamforming array must have (>8cm per side for a minimum 2x2 array, determined by simple physics) it is important not to over- or under-specify it, otherwise usability of GRABEL could be impacted too heavily. The specifications given here will then be refined during the GRABEL development and should be reflected in its manual or data sheet.

**Keyword list:** *GNSS receiver, Reconfigurable antenna, beamforming techniques*

## Executive Summary

Global Navigation Satellite Systems (GNSS) are expected to form a major part of the so-called 4G picture, providing the citizen with truly positioning and Localization Based Services (LBS). The GRABEL project is investigating a new GNSS receiver concept, deriving its main characteristics, which mainly concern a novel receiver architecture that jointly exploit a reconfigurable antenna and an adequate baseband processing in order to significantly enhance the GNSS receiver performance (localization accuracy and LBS reliability).

The main objective of this deliverable is to provide the system specification of the GRABEL integrated framework. This is performed on the basis of analyzing and accessing the overall requirements specified in deliverables D1.1 to D1.3.

An implementation-oriented approach will be followed for the clustering of the GRABEL specified sub-systems and concepts. The particular work items addressed in the context of this deliverable concern the specification of the following technological aspects:

1. *Generic Architecture*: In this context, the classes of supported applications, are specified in order to define the GRABEL targeted framework.
2. *Structure of the antenna system*: relating to the specification of the various parameters needed for the intended reconfigurable antenna design, including the number of antenna elements, the antenna polarization exploitation, the placement of the antenna elements...
3. *Structure of the GNSS receiver*: including required parameters such as frequencies, bandwidths, dimensions...
4. *Architecture of the baseband processor*: with specific features including HW / SW partitioning, Beam forming or diversity, Type of beam forming (pre- vs. post-correlator, if any) , Type and number of search and tracking engines...
5. *Mechanical aspects of GRABEL receiver*
6. *Application software*

Once the various GRABEL conceptual and functional elements have been specified to an adequate extent, the specification of the demonstrator principles will follow up.

## Table of contents

<b>1</b>	<b>INTRODUCTION</b>	<b>7</b>
<b>2</b>	<b>ARCHITECTURE AND SYSTEM SPECIFICATIONS</b>	<b>8</b>
2.1	SPECIFICATION OF THE 2 SELECTED AND TARGETED APPLICATIONS	8
2.1.1	<i>Semantics-based Near Indoor Navigation Application</i>	8
2.1.2	<i>A Near-Indoor Search-and-Rescue Application</i>	10
2.2	STRUCTURE OF THE ANTENNA SYSTEM	13
2.2.1	<i>Working with Reconfigurable antenna</i>	15
2.2.2	<i>Reconfigurable antenna geometry</i>	16
2.2.3	<i>Achieving polarization diversity</i>	18
2.2.4	<i>Reconfigurable antenna "edge" miniaturization</i>	19
2.2.5	<i>Discussion on SPA padding in arrays</i>	24
2.2.6	<i>Determining the antenna's distance in the array</i>	27
2.2.7	<i>Placement and number of antennas – spatial configuration</i>	30
2.2.8	<i>Results and candidate selection</i>	36
2.2.9	<i>GRABEL antenna system</i>	38
2.3	ARCHITECTURE OF THE BASEBAND PROCESSOR	41
2.3.1	<i>HW / SW partitioning</i>	41
2.3.2	<i>Beam forming or diversity</i>	41
2.3.3	<i>Type of beam forming (pre- vs. post-correlator, if any)</i>	48
2.3.4	<i>Measurement and navigation engines</i>	50
2.4	MECHANICAL ASPECTS OF GRABEL RECEIVER	53
2.5	APPLICATION SOFTWARE	55
2.5.1	<i>Application Software for GRABEL Receiver</i>	55
2.5.2	<i>Application Software for Semantic Processing</i>	56
2.5.3	<i>Implementation of the Application Software</i>	56
<b>3</b>	<b>CONCLUSIONS/SUMMARY</b>	<b>57</b>
<b>4</b>	<b>REFERENCE DOCUMENTS</b>	<b>58</b>
<b>5</b>	<b>BIBLIOGRAPHY</b>	<b>58</b>

## List of figures

Figure 1.1: Localization method	7
Figure 2.1: Specification of the near-indoor semantic navigation application	9
Figure 2.2: Sequence diagram for the near-indoor semantic navigation application	10
Figure 2.3: UML Component diagram for specification of the near-indoor search and rescue application	11
Figure 2.4: UML Sequence diagram for the near-indoor search and rescue application	12
Figure 2.5: Basic architecture of a linear array of sensors.	13
Figure 2.6: Array configurations with different number of elements and $d/\lambda$	14
Figure 2.7: GRABEL antenna PoC system proposed preliminary schematic	15
Figure 2.8: GRABEL antenna system prototyping approach	16
Figure 2.9: Array of three parallel half-wavelength dipoles loaded with impedances $Z_{L2}$ and $Z_{L3}$ (a) and equivalent Z-matrix circuit model (b).	16
Figure 2.10: Simulated (solid) and measured (dashed) radiation patterns for the two states.	17
Figure 2.11: Simulated and measured return loss in the first state: Nearly identical results are obtained in the ON-OFF state.	17
Figure 2.12: Vertical miniaturisation of SPA using higher dielectric substrate and meanderization	18
Figure 2.13: SPA antenna with dual polarization	19
Figure 2.14: side view of SPA with reflector and top view of WLAN prorotype.	19
Figure 2.15: GRABEL 3x3 Switched parasitic antenna (left) with approximate size at GPS L1 frequency (center) and edge antenna miniaturization opportunity (right) with vertical plate shortcuts.	20
Figure 2.16: Edge antenna miniaturization opportunity (side cut)	20
Figure 2.17: Alternative Single pole four through (SP4T) using four highly decoupled corner antennas	20
Figure 2.18: Variant of Electronically Steerable Passive Array Radiator (ESPAR) antennas	21
Figure 2.19: "Classical" Phased array using twelve elementary sources.	22
Figure 2.20: "Array using four reconfigurable cells having each a reconfigurability capacity for a global similar directivity.	22
Figure 2.21: Inline and quincunxes WLAN arrays of SPAs	22
Figure 2.22: "Adaptive antenna based on four reconfigurable cells (a) and reconfigurable cell using patch as radiating elements (b).	23
Figure 2.23: RF MEMS based beamforming array [Peti07]	24
Figure 2.24: Achievable radiation pattern with two elements switched parasitic antenna (SPA-2)	24
Figure 2.25: Different order of SPA from SPA-2 to SPA-6	25
Figure 2.26: Assembly of SPA-4 in 5 active elements array (overall dimension 30x30cm)	25
Figure 2.27: Assembly of 1 SPA-6 in 4-5-7 active elements array (larger dimension are respectively 15-30-37-45 cm)	26
Figure 2.28: 3x3 array using classical "isotropical" sources and SPA-4 array equivalent to parasitic antenna element interleaving	26
Figure 2.29: General system block diagram	38
Figure 2.30: Complete antenna array (right), antenna array subset for the selected configurations (left)	38
Figure 2.31: SPA MEMtenna concept and detail of the parasitic antenna impedance loading	39
Figure 2.32: 5x5 patch antenna array (left), MEMtenna unit cells (centre), achievable 3x3 MEMtenna array	40
Figure 2.33: Beam former implemented analogically at the RF level	42
Figure 2.34: Concept of multilevel beamforming (Analogue and digital)	43
Figure 2.35: Concept of digital beam former implementation	43
Figure 2.36: Selection diversity	44
Figure 2.37: Maximal Ratio Combining	44
Figure 2.38: Equal Gain Combining	45
Figure 2.39: Narrowband Beamforming	46
Figure 2.40: Generalized Side lobe Canceller (GSC)	47

---

<i>Figure 2.41: Pre Correlation with samples buffering</i>	49
<i>Figure 2.42: Pre Correlation with phase controlled by NCO</i>	49
<i>Figure 2.43: Tracking engine and navigation filter processes</i>	51
<i>Figure 2.44: GRABEL antenna system integrated in laptop screen holder</i>	53
<i>Figure 2.45: GRABEL antenna system externally connected</i>	53
<i>Figure 2.46: GRABEL roof mounted antenna system for emergency vehicle in urban canyon environment</i>	54

## List of tables

<i>Table 2.1: Dual axis SPA reconfigurable antenna using DIME or PP miniature antenna</i>	21
<i>Table 2.2: 2 antenna isotropic beam patterns (<math>d = 0 - 4\lambda</math>)</i>	27
<i>Table 2.3: Table of GNSS frequencies</i>	28
<i>Table 2.4: 2 antenna isotropic beam patterns (<math>d = 0.09515m</math>)</i>	29
<i>Table 2.5: 2 antenna isotropic beam patterns (<math>d = 0,11010m</math>)</i>	30
<i>Table 2.6: Key points of antenna configuration study</i>	31
<i>Table 2.7: Single antenna</i>	31
<i>Table 2.8: Inline array of antennas</i>	31
<i>Table 2.9: Antennas disposed in a square</i>	32
<i>Table 2.10: 2 crossing antenna array</i>	33
<i>Table 2.11: Triangular and hexagonal configuration</i>	34
<i>Table 2.12: 3D simulation of 2x2 square and 9 antennas cross configurations</i>	35
<i>Table 2.13: Spatial configuration vs. number of parameters</i>	36
<i>Table 2.14: Number of antennas vs. matrix complexity and parameters</i>	37
<i>Table 2.15: Best candidate antenna arrangement retained for further testing</i>	37
<i>Table 2.16: Comparison of different beamforming algorithms [4]</i>	41
<i>Table 4.1: GRABEL reference documents</i>	58
<i>Table 5.1: Bibliography</i>	58

## 1 Introduction

GRABEL is an SME research initiative intended to investigate the joint use of reconfigurable antennas and beamforming algorithms for the purpose of improving the localization capabilities of Global Navigation Satellite systems (GNSS) receivers (including GPS and Galileo) in outdoor and light-indoor propagation environments. As such, the localization method illustrated in figure 1.1 will lead to better localization performance (localization accuracy and LBS reliability).

The main tasks carried out in deliverables D1.1 to D1.3 comprised the identification of the overall system requirements, both functional and non-functional, investigation for potential “boundaries”, outline of a high level architecture, and performing a critical analysis for assisting towards a consistent functional and technical system specification. Overall system requirements originate in the envisaged GRABEL concept, the technological state of the art, and the general market-derived requirements. The latter are characterized by: existing market needs; state of the art and trends; other influential market-derived, social, and technological factors. The collection and analysis of the overall market-derived requirements provide the means for the definition of a more implementation-oriented set of system requirements. These are categorized in functional ante baseband processing.

The main objective of this deliverable is to provide the system specification of the GRABEL integrated framework. An implementation-oriented approach is followed for the clustering of the GRABEL specified sub-systems and concepts.

System specification will provide the guidelines for future development and research activities. Technical work in the context of GRABEL will be focused on two main aspects of the envisaged functional framework:

- 1) The design and optimization of the reconfigurable antenna that will be used in the GNSS receiver.
- 2) The investigation and implementation of high-level baseband processing algorithms that will drive the reconfigurable antenna.

Regarding the two category of activities, an innovative and adequate design and optimization methodology will be specified. Demonstration of the research and development outcomes will be performed in a first step mainly by means of simulation.

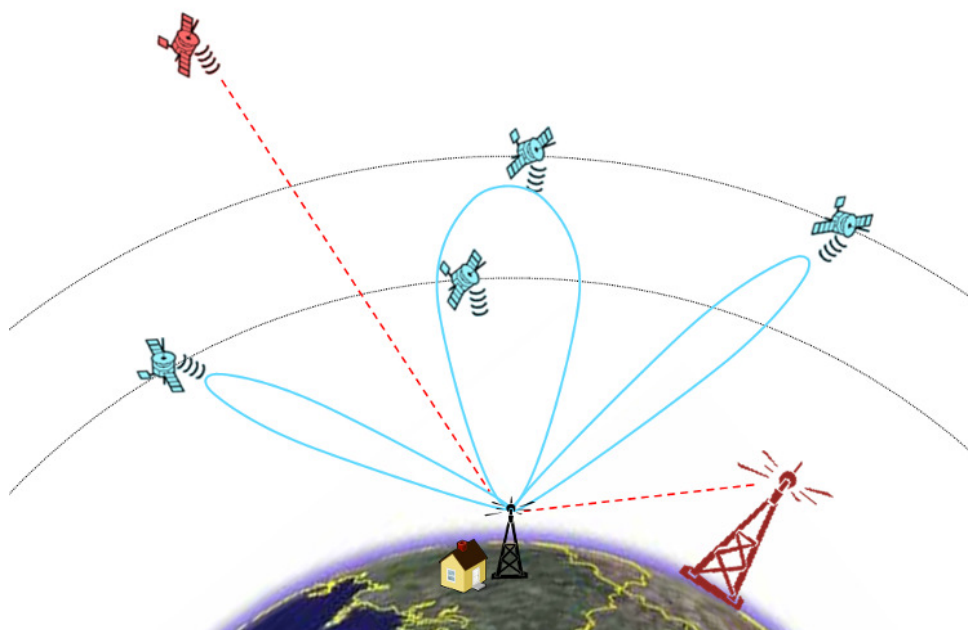


**Figure 1.1: Localization method**



## 2 Architecture and system specifications

The purpose of deliverable D1.4 is to specify the GRABEL receiver as much as possible. It shall be meant basically as a datasheet of T1.3. If unresolved trade-offs remain, the basis to solve them is at least given here.

### 2.1 Specification of the 2 selected and targeted applications

#### 2.1.1 Semantics-based Near Indoor Navigation Application

The first application refers to an integrated near-indoor navigation system, which is based on modelling both geometric and semantic structure of near-indoor environments. The description of this application and a scenario is described in D1.2. By using this application, handicapped users can obtain navigation paths and guidelines that match to their physical and perceptual capabilities. The specification of this application is achieved with defining the UML functional component of the application and depicting its functionality through a UML sequence diagram.

##### 2.1.1.1 Specification of the Components

The user first has to define his/her capabilities of moving, preferences for navigating from one place to another, e.g., the minimum distance, or the path with accessible passages /ramps due to the wheelchair. This means that, the user specifies his/her navigation profile along with his/her destination. The current exact position is detected by the GRABEL receiver. Hence, the input to the application is the user-capability profile, the current place and the destination.

Upon request, the application attempts to find a set of paths that match the user profile w.r.t. the current (starting) and destination points. For each possible path, the user can select one that prefers. On his/her way on the selected path, the application informs continuously the user about the current itinerary and the next passages or points of directions until the end of the route.

As described in D1.2, the functional components for this application are:

**Navigation Service::Navigation Interface.** This service is the interface between the application and the handicapped user. Specifically, there is a friendly user interface with which the user can create his/her navigation profile and provide information about the targeted destination. The response of such interface is the optimal path, if any, which optimality depends on the suitability for current user context and length of the selected paths. In addition, through this interface, the user is constantly being informed about his/her position on the selected route from the starting point to the destination. Finally, several guides are displayed on the user's display regarding the navigation plan.

**Navigation Service::Profile Manager.** The user navigation profile is managed by the Profile Manager. This component maintains data for modeling the user capabilities, constraints and preferences into the User Navigation Ontology (UNO). Based on the inserted/declared capabilities, the user is classified into one or more capabilities classes according to his/her characteristics. Such classification is used by the application in order to find the optimal set of paths. In addition, the Profile Manager maintains the NINO ontology (Near-Indoor Navigation Ontology). This spatial ontology maintains the basic spatial and structural concepts of near-indoor environments, as well as their relationships. Such concepts are adopted in the UNO ontology in order to describe the preferences of a user, for instance, the user prefers to reach his/her destination avoiding elevators but using ramps. The elements ramps and elevators, their position along the path and their operation are described in the NINO ontology. The NINO instances are created through a geometric representation of the near-indoor topology. Such geometric data may initially reside in a Geographic Information System (GIS) as building blueprints and be, subsequently, transformed to actual spatial ontology instances. We can assume that the NINO instances have been created beforehand and thus, do not delve into the details of such creation process.

**Navigation Service::Near-Indoor Positioning System.** This sub-system is invoked by the navigation interface in order to symbolically locate the users in the navigation space according to the spatial model described by NINO. In addition, once the user has selected a path and navigates along this

path, the positioning sub-system monitors the current user position and the Navigation Interface displays his/her trace on the device's display.

**Navigation Service::Path Selection Algorithm:** The path selection process is performed through a set of rules. The definition of such rules involves the spatial semantics (*i.e.*, spatial relationships expressed through the NINO ontology) and the user semantics (*i.e.*, user capability of movement/preferences/profile expressed through the UNO ontology). The rules are applied to the NINO instances in order to determine the paths that are considered appropriate and accessible for each user request. Finally, the algorithm returns *k-shortest paths* with the meaning that the shortest path is not always the optimal path, e.g., the shortest path can satisfy all the user restrictions w.r.t. user navigation profile.

### 2.1.1.2 UML Component and Sequence Diagram for Specification

The following UML Component Diagram shown in figure 2.1 depicts the abstract component specification for the near-indoor navigation service.

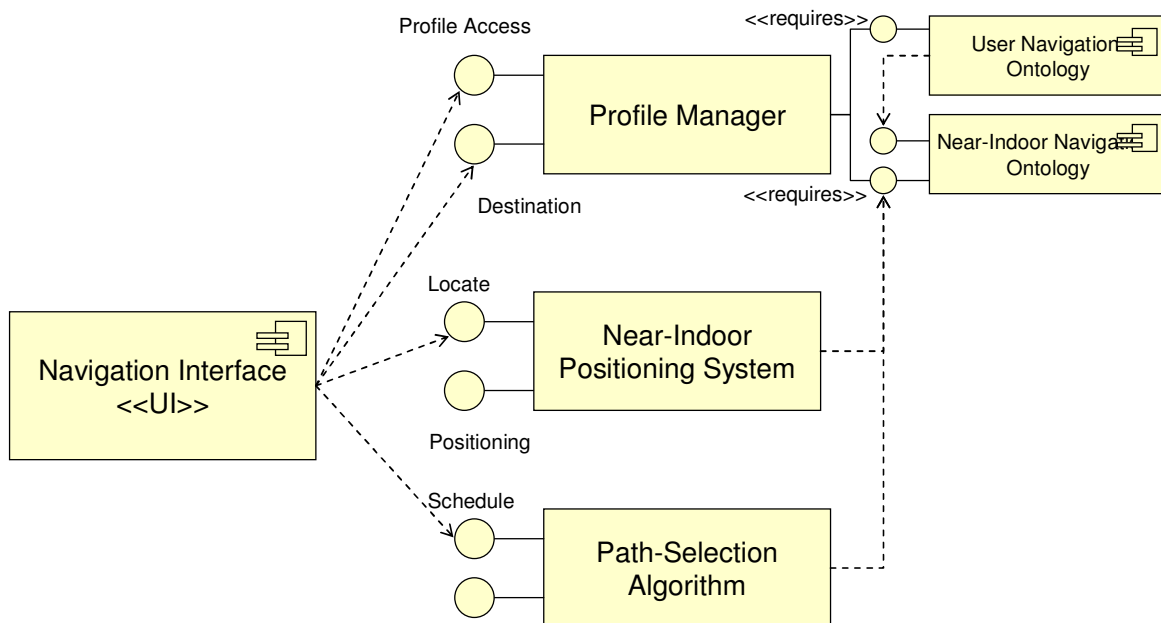


**Figure 2.1: Specification of the near-indoor semantic navigation application**

The Navigation Interface component accesses the Profile Access and the Destination interface of the Profile Manager component in order to define and set the user navigation profile and the parameters for a route (destination). The starting point and, in general, all the localization of the user is provided by the Locate interface of the Near-Indoor Positioning System. The latter accesses the NINO ontology for displaying not only the current position of the user but also the spatial elements during the navigation of the user. The Path-Selection Algorithm component uses both ontologies in order to support the user with a set of the optimal routes/paths w.r.t. the navigation profile and the operational status of certain spatial elements (e.g., route is closed for construction, external elevator is not in operation, ramp is steep, etc.).

The Sequence Diagram shown in figure 2.2 depicts the specification functionality of the application dealing with a navigation request. Specifically, the Navigation Service initiates a new user navigation profile or/and creates a session for a specific route (starting point and destination). The Profile Manager sends to Navigation Service the exact symbolic location in the map for the starting point, the destination point and the specific spatial elements for any selected path. Such localization is achieved by the Positioning System. The Path-Selection Algorithm returns a set of the optimal paths according

to the user navigation profile to the Navigation Service. Once the user has selected the preferable route then the Positioning System (i) monitors the user orientation and way to the destination (ii) updates regularly the display of the Navigation Service with up-to-date information for the current position of the user and the status of the spatial elements of the route.

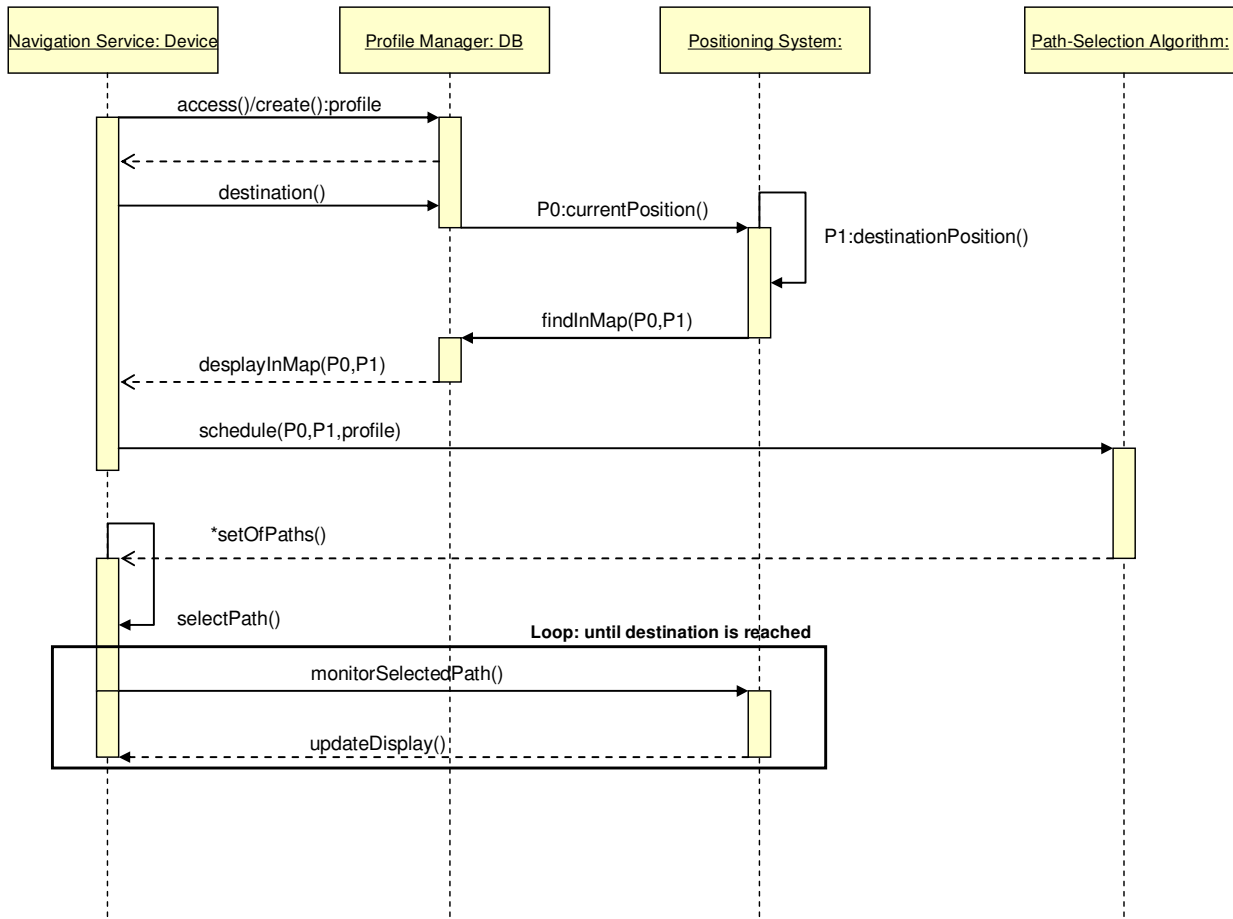


Figure 2.2: Sequence diagram for the near-indoor semantic navigation application

## 2.1.2 A Near-Indoor Search-and-Rescue Application

The second application refers to a Near-Indoor Search-and-Rescue (NISAR) application. The high value of position accuracy and the continuity for the position service provided by the GRABEL receiver are crucial requirements for such SAR application. In this application a set of small rescue robots can be equipped with specialized sensors capable of detecting human victims in buildings after earthquake oscillations. In totally collapsed buildings there is no infrastructure for communication among the rescue team and possible victims. The following components specify the functionality of the SAR application.

### 2.1.2.1 Specification of the Components

The rescue robots are equipped with a set of seismic, location and acoustic sensors. The sensed information at time instant  $t$  is recorded (time-sampling) to the **Sensing Component (SC)**. That is the SC maintains records of sensed data  $\mathbf{v} = [\text{noise, vision, longitude, latitude, time}]$  that is recorded constantly as long as the rescue robot explores the near-indoor area.

The sensed data can be processed on-line or a post-processing procedure can be initiated by the rescue team by the **Processing Component** (PC). In the first case, due to eliminated infrastructure - totally damaged - of the collapsed building, the robot can send regularly sensed values  $\mathbf{v}$  at time  $t$  through a wireless interface of the SC to the PC for further decisions on the rescuing procedure. In the latter case, the recorded data of the SC is analyzed by the rescue team after the exploration of the robot(s). Once the  $\{\mathbf{v}(t)\}$  set of values is analyzed, the rescue team can define a rescue plan, like find the path and locate the position of the trapped persons, for a rescue mission.

The rescue team is provided with a **Navigation Service component** (NS) which displays the position of the rescue robots and attempts to illustrate possible area in the totally collapsed buildings with trapped persons into ruins. The NS communicates with the SC in order to depict the traces of the robots and, after the processing of the PC, the NS updates the illustration of the display with the possible areas for further exploration. This also implies that, the NS can rank areas of the collapsed building along with the probability of finding trapped persons.

### 2.1.2.2 UML Component and Sequence Diagram for Specification

The following UML diagram in figure 2.3 depicts the three components of the SAR application. The NC provides a navigation interface which displays the traces of the rescue robots (provided by the Display Traces interface of the PC) and the deduced possible areas in which the probability of existing trapped persons is high (provided by the Illustrate Areas interface of the PC). The PC exploits On-line Streaming and Asynchronous Recording interfaces of the SC. Specifically, the former interface is used to capturing up-to-date the sensed data of the robot exploration including the position of the robot. In case there is no wireless communication between the PC and the SC then the PC exploits the recorded sensed data after the exploration of the robots through the Asynchronous Recording interface. The SC requires communicating with the set of the equipped sensors on the rescue robot for retrieving and stopping the sensing process. This is achieved by the Publish and Stop Sensing interfaces of the real sensor device.

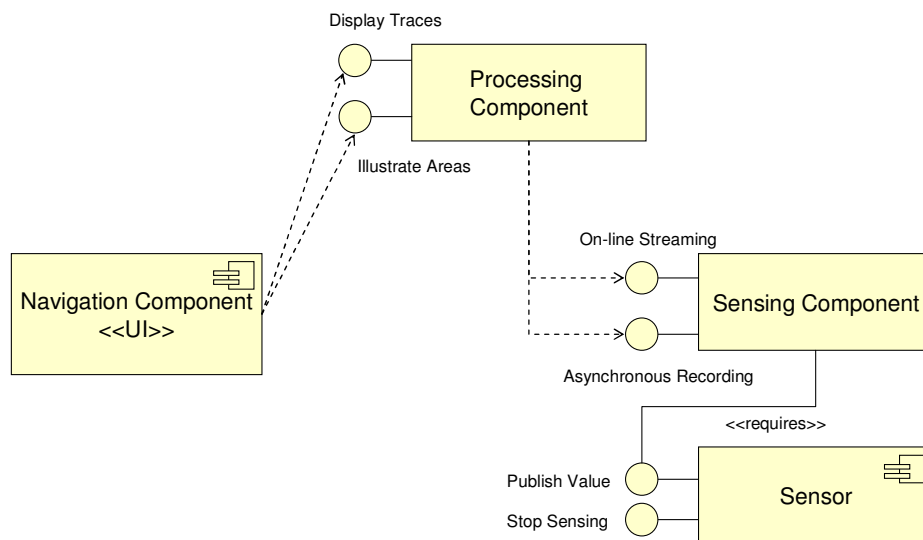


**Figure 2.3: UML Component diagram for specification of the near-indoor search and rescue application**

The following figure 2.4 depicts a sequential diagram of the functionality of the components of the SAR application. The NC requests for displaying the robot-traces and the possible areas for further exploration of focus of the rescue process. The PC communicates with the SC on-line in order to capture the current position of the robot and either synchronously receives the sensed data or asynchronously receives the stored data from the SC. The UML diagram depicts those two different way of processing the sensed data in order for the rescue team to acquire a rescue map the displays

(i) the traces of the robots that had followed in order to find trapped persons and (ii) the possible areas in the collapsed buildings that report trapped persons with high probability in a ranked order.

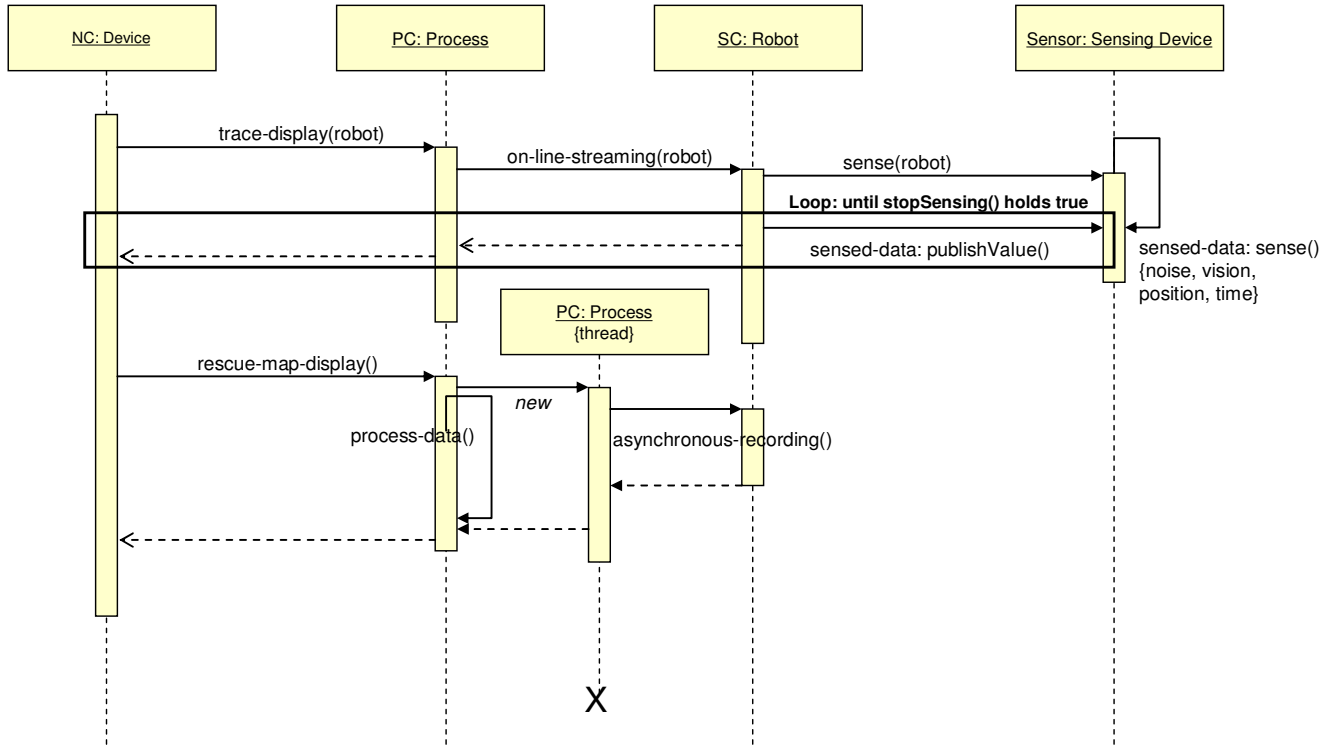


Figure 2.4: UML Sequence diagram for the near-indoor search and rescue application

## 2.2 Structure of the antenna system

We can consider a phased array of antennas as a spatial filter, as opposed to a temporal filter, where the output (the beam) depends on the number of antennas and their displacement. The angular width of the main lobe (3-dB beam width), in its far field radiation pattern, is related to the number, spacing, shape and size of the sensors array. For instance the half power beam width for a linear array with uniform weighting is  $HPBW=0.88\lambda/A$ , where  $A$  is the aperture length of the array  $A = N d/\lambda$  ( $N$  the number of sensors). This way the higher are both the number of sensors  $N$  and the size of the array and the narrower is the beam. Care must be taken to minimize the grating lobes in addition to the desired main lobe created by large spacing of the array elements. In principle a beam of an array is formed adjusting in a proper manner the phase (or time delay if the array is large). In the adaptive beamforming mode the amplitudes weight need to be adjusted, on the base of the algorithm used, as well.

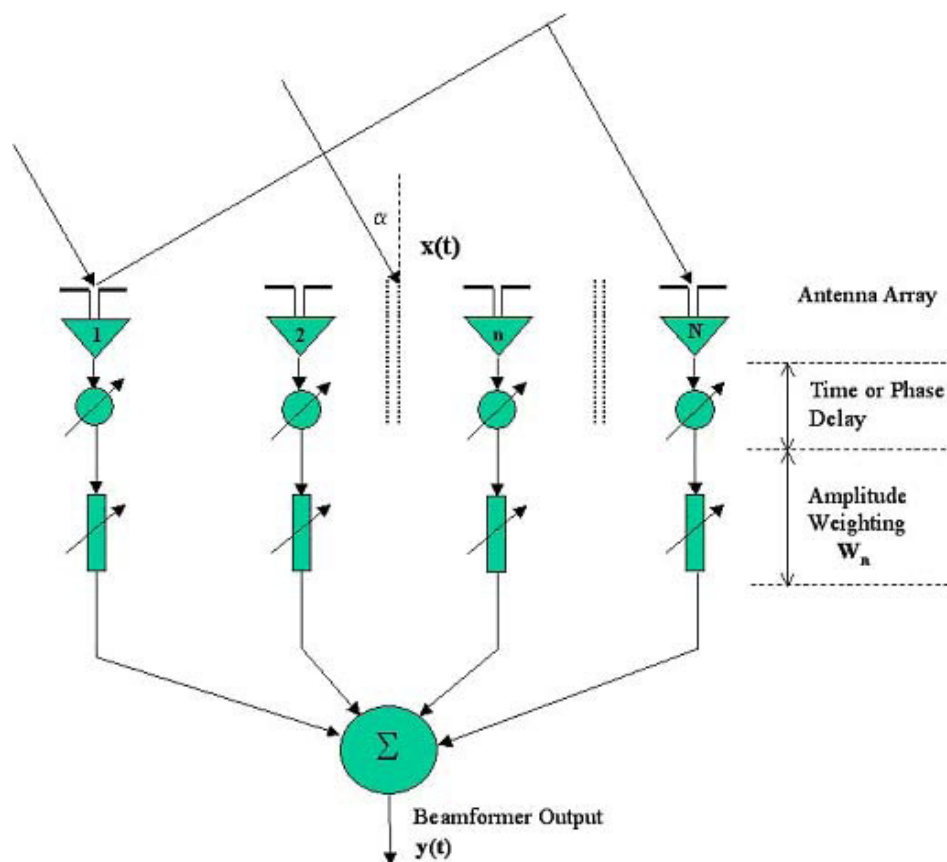


Figure 2.5: Basic architecture of a linear array of sensors.

An idea on the dependence (i.e. for a linear array) of the beam shape in a plane, from both the number of antennas and the distance [3], is visible in figure 2.6. Of course the same considerations can be done for a 2D array (in the space).

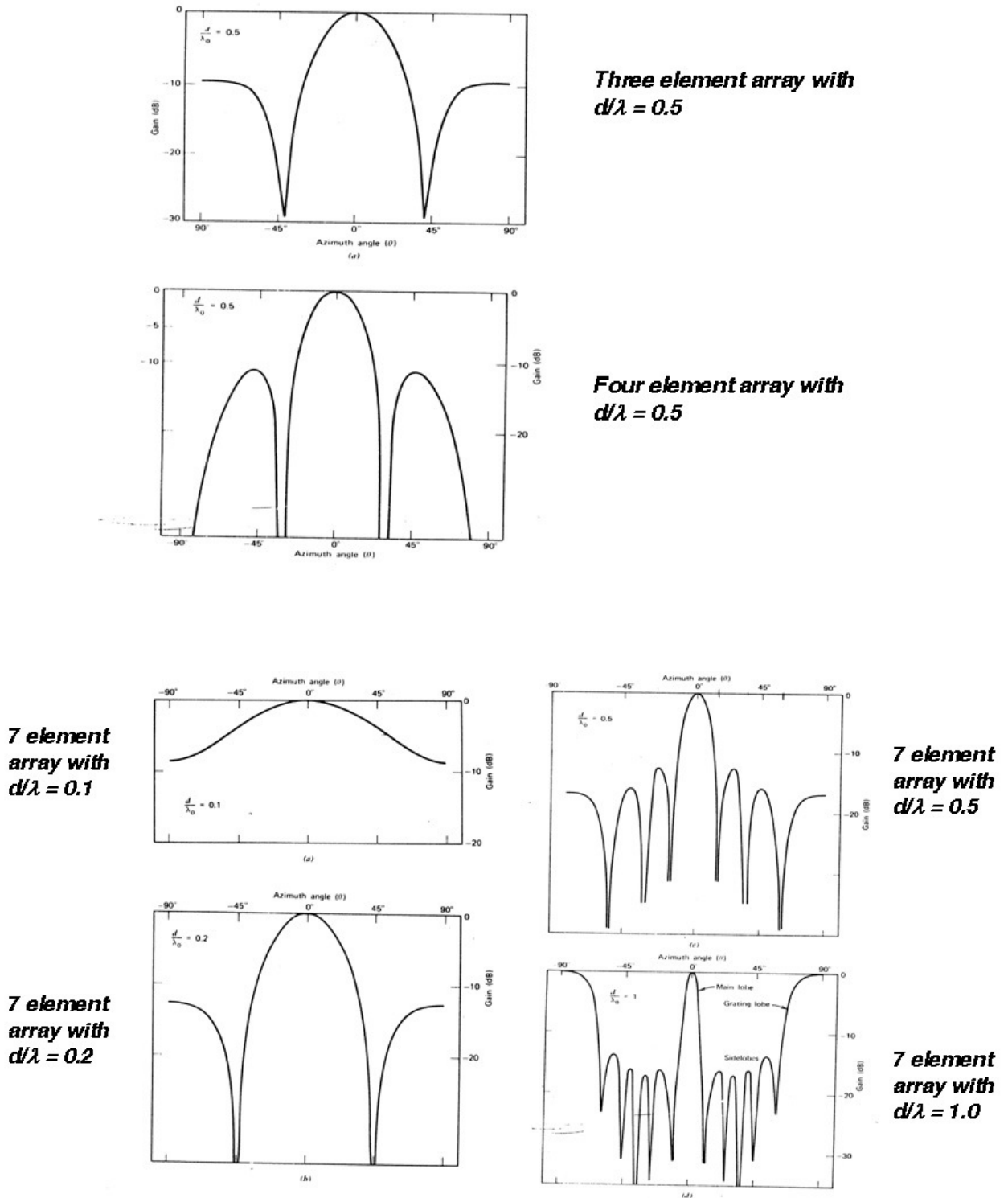


Figure 2.6: Array configurations with different number of elements and  $d/\lambda$ .

In the adaptive beamforming mode the number of sensors  $N$  limits the number of interferers that can be pointed with the zeroes of the beam pattern. Theoretically such a number is  $N-1$  but with some distortion of the beam shape, in practice in a large number of sensors is possible to point  $N/2$  interferers without beam shape degradation. Same considerations are valid for a 2D array.

### 2.2.1 Working with Reconfigurable antenna

The motivation for using MEMtenna, i.e. reconfigurable antenna unit cells, in the frame of the GRABEL advanced receiver architecture has been extensively discussed in D1.1. GRABEL stand for GNSS reconfigurable antenna based enhanced localization. A reconfigurable antenna is a radiator which has the particular capability to change its fundamental operating characteristics (radiation pattern, frequency or polarization) through electrical, mechanical or other means.

The MEMtenna is a reconfigurable antenna using MEMS, Micro Electronic Mechanical systems actuators to reshape its size and shape in order to change its characteristics, or integrate in some specific place RF MEMS components (see GRABEL D1.1). GRABEL particularly target the development of RF MEMS or RF solid state component based reconfigurable antenna.

One of the GRABEL main motivations is thus the use of such MEMS based reconfigurable antenna, alone or as unit cell of broader antenna system, in order to enhance the localization.

As Described in D1.1. an active RF feed networks with N lines for N active antenna (N=2...16 as described in 2.2.1 of this document) is quite complex. It is envisaged for professional applications such as geodetic applications. But more mass market that GRABEL SMEs are targeting the integration of one Single active antenna with surrounding passive parasitic antenna is more appropriate. Alternatively multiantenna with limited number of antenna (2-4) might be envisaged for smaller application.

The principle of operation of the PoC Antenna system is a Switched parasitic antenna version is to have one main antenna, possibly active, and shape the radiation pattern thanks to close coupled "parasitic" elements, between third and quarter lambda ahead from main antenna.

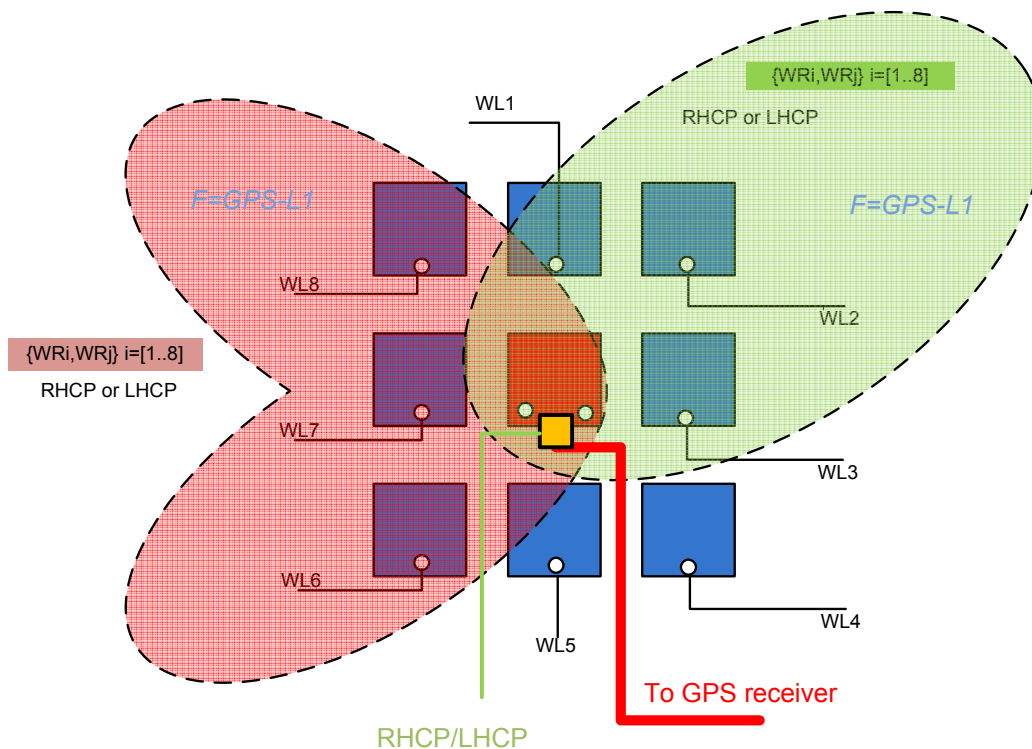


**Figure 2.7: GRABEL antenna PoC system proposed preliminary schematic**

Within GRABEL, the antenna system design and prototyping would first demonstrate the system PoC with from factors that are more important like laptops or PDAs.



The final dimensions of the GRABEL receiver will be conditioned by the number of antennas needed to reach the improvement targeted in the project.

The aforementioned consideration about prototyping is illustrated in the figure 2.8 below.

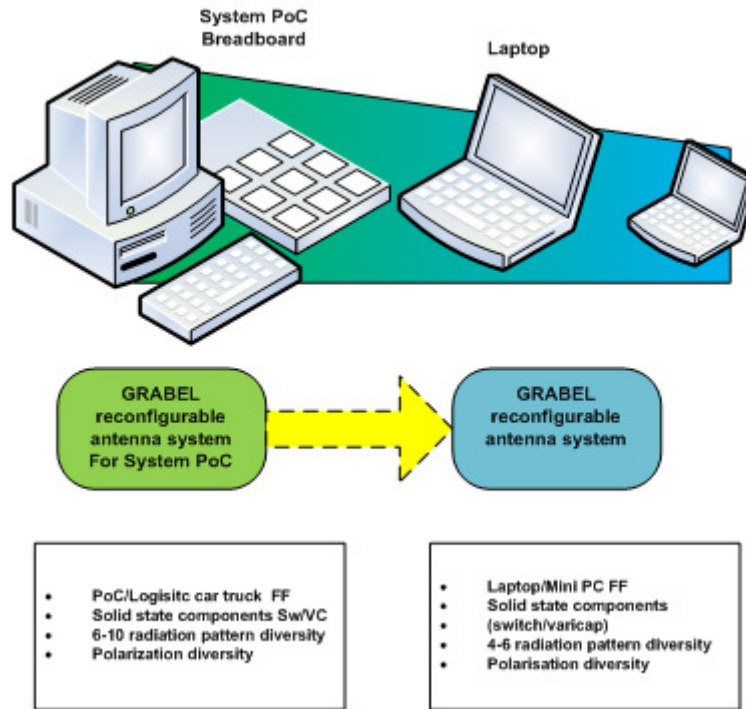


Figure 2.8: GRABEL antenna system prototyping approach

### 2.2.2 Reconfigurable antenna geometry

As a reminder one suitable reconfigurable antenna is the switched parasitic antenna. This provide sufficient radiation pattern shaping to mitigate the influence of multipath in several directions.

In [Pet06], we presented new modeling method of parasitic antenna arrays suitable used to design a MEMS-switched parasitic antenna array at 5.6 GHz using stand-alone packaged series MEMS switches. Experimental results were in good agreement with the simulations, providing two switched beams at  $\pm 25^\circ$ . In [Pet06] the RFMEMS were developed by LETI for the French Space Agency (CNES): we acknowledge here again their support for the development of MEMS-switches.

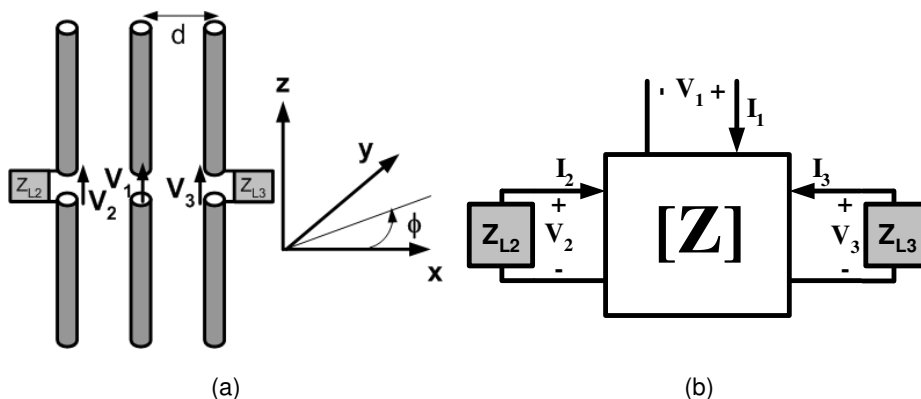
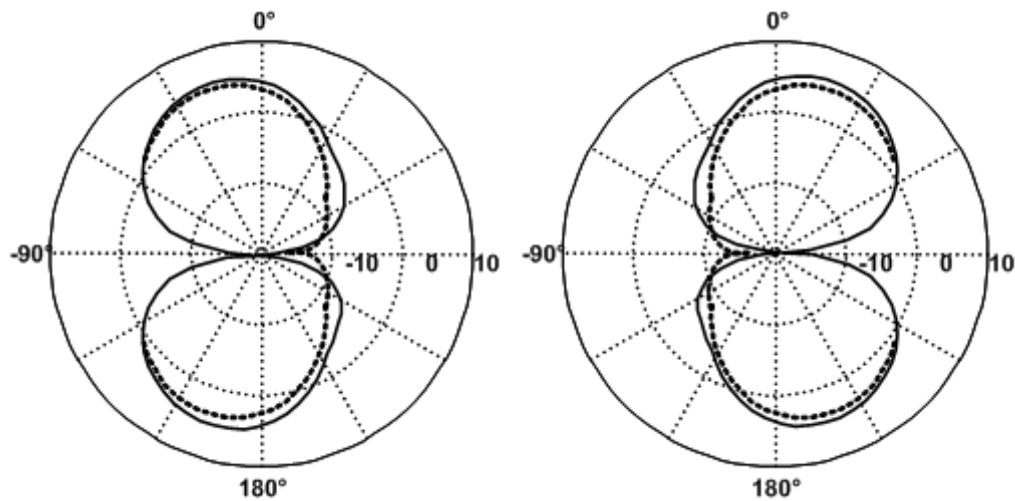
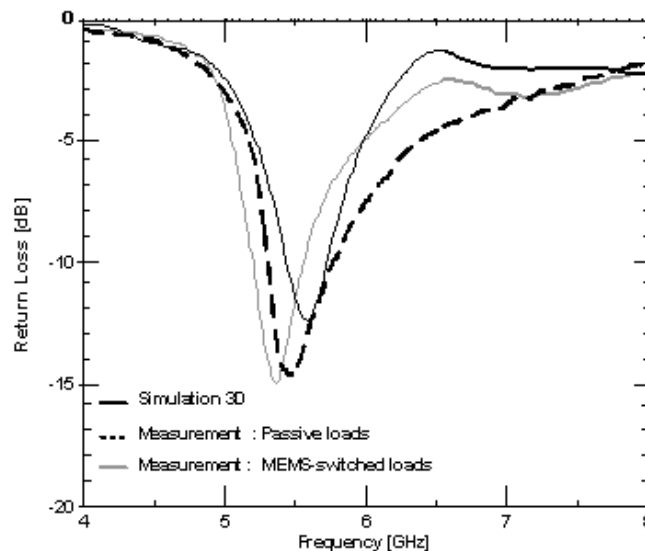


Figure 2.9: Array of three parallel half-wavelength dipoles loaded with impedances  $Z_{L2}$  and  $Z_{L3}$  (a) and equivalent Z-matrix circuit model (b).



**Figure 2.10: Simulated (solid) and measured (dashed) radiation patterns for the two states.**



**Figure 2.11: Simulated and measured return loss in the first state: Nearly identical results are obtained in the ON-OFF state.**

Radiation pattern diversity antennas are expected to result in improved performances for wireless applications in perturbed environments. GNSS outdoor, light indoor signal as in the frame of GRABEL is such highly multipath propagation environment.

In terms of geometry, the spacing  $d/\lambda$  between the central RF element and the parasitic elements can cover values between 0.2 and 0.5, see also section **Error! Reference source not found., Error! Reference source not found.** The switched parasitic antenna design will be impacted in such way. The closest the elements the highest the coupling factors, but on the other hand, having more spaced elements helps in achieving radiation pattern diversity. But having the parasitic elements too far away (e.g.  $d/\lambda=0.6$ ) would degrade so much the coupling factors, that the achievable radiation pattern diversity will be less interesting. A good trade off for achieving radiation pattern diversity is, given our experience, between  $d/\lambda=0.27$  and  $d/\lambda=0.32$ . It is possible to achieve the design miniature antenna as small as  $\lambda/20$  especially for narrow band systems such as GPS-L1 systems (some tens of MHz at 1575 MHz). This would then drive us to a SPA (Switched Parasitic Antenna) length of  $0.54 \lambda$  for one central element (that's 103mm). But practically speaking the achieved minimum length would rather be 120 mm. The theoretical height of such SPA is slightly bigger than half wavelength slot which in air would be, 120 mm as well. But the slot will be designed on woven glass with resin substrate (e.g. FR4) or Teflon material, or even ceramic based substrate. The guided wavelength in such substrate is divided by the square root of the relative permittivity. For the afore mentioned substrate, which relative

permittivity covers value in between 1.5 and 10 this could lead to size reduction in height of over 3 times leading to a form factor of 120x40mm.

Nevertheless, we would probably use classical substrate with permittivity in the order of 4 such as FR4. Anyway, having substrate with too high permittivity, will effectively reduce the length of the radiator, but will also meanwhile degrade their radiation efficiency.

This would then lead us to a form factor of 120x60 mm. In addition to substrate, many other miniaturization techniques could be used such as meanderization, wire-patch, PIFA/IFA, etc.. , leading to theoretical limit of  $d/\lambda=1/20$ . This would then lead to a one axis SPA with form factor of 120mmx40mm. A clear multipath and interferer's rejection will be kept. But for a combined SPA in XX' axis and SPA in YY' axis, or any further combination (e.g. parasitic hexapole, parasitic octopole), the size of one MEMtenna would reach 120x120mm.

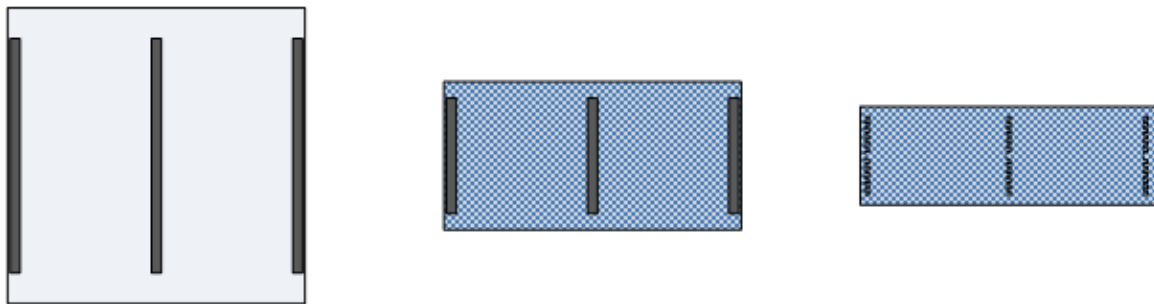


**Figure 2.12: Vertical miniaturisation of SPA using higher dielectric substrate and meanderization**

### 2.2.3 Achieving polarization diversity

The network of antenna with three parasitic elements presented before product a radiation pattern with a simple polarization. However, it was shown that the diversity of polarization is strongly desirable in highly multipath environment. Such polarization diversity can be achieved using dual axis, where the two structures were combined. On this principle, two cross antennas derived from the antenna containing slits presented previously were developed. These antennas bring not only a diversity of diagram but also a diversity of polarization thanks to actuation of a SPDT switch (Individual-Pole-dual-Throw). The figure below show a two axis antenna realized for WLAN application [Pet07].

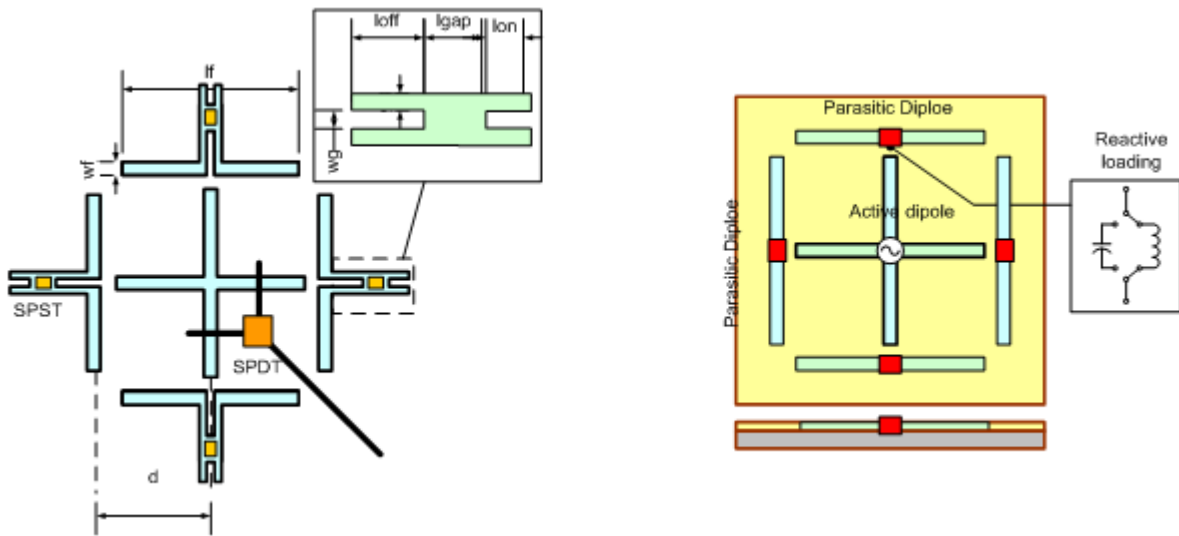


Figure 2.13: SPA antenna with dual polarization

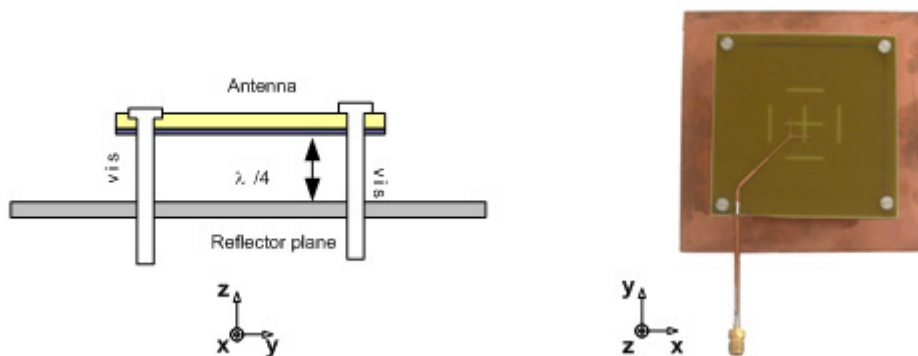
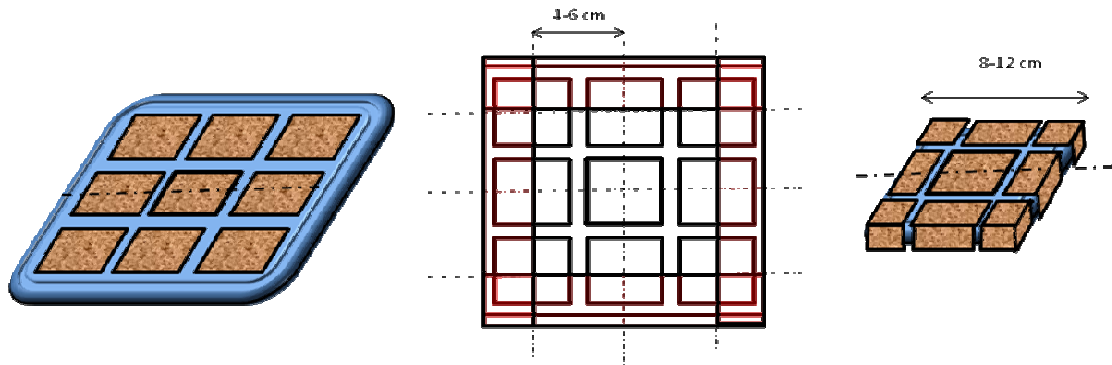


Figure 2.14: side view of SPA with reflector and top view of WLAN prototype.

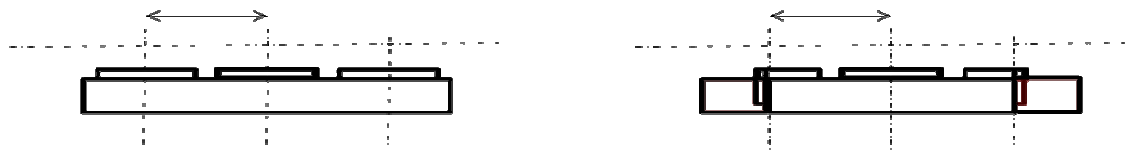
### 2.2.4 Reconfigurable antenna “edge” miniaturization

The principle of operation of the Switched parasitic antenna version is to have one main antenna, possibly active, and shape the radiation pattern thanks to close coupled “parasitic” elements, between  $\lambda/3$  and  $\lambda/4$  ahead from main antenna. At GPS-L1, ( $f=1575.42$  MHz) that means 4 - 6 cm spacing distance between active antenna and parasitic antenna phase centre.

As we ultimately target the integration of MEMS based variable loadings on parasitic antenna, we name them as MEMS based antenna or MEMtenna. As a matter of fact we first target the integration of solid state devices. The preconception of the GRABEL 3x3 Switched parasitic antenna is presented on figure 2.15. The same figure also shows the derivation of this MEMtenna towards a more compact version using edge antenna miniaturization opportunity (right) with vertical plate shortcuts (figure 2.16).

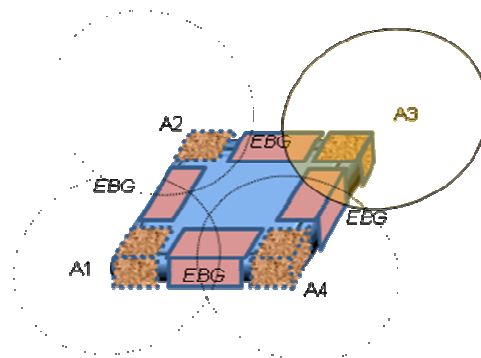


**Figure 2.15: GRABEL 3x3 Switched parasitic antenna (left) with approximate size at GPS L1 frequency (center) and edge antenna miniaturization opportunity (right) with vertical plate shortcuts.**



**Figure 2.16: Edge antenna miniaturization opportunity (side cut)**

Additionally the radiation element can be any antenna, patch slot. In order to achieve a higher order of integration we would also evaluate much advanced miniaturization techniques such as IFA/PIFA, miniature DIME, meandered or their combination. An alternative way to design the GRABEL reconfigurable antennas, particularly suitable for small devices would be to use separate antenna with clearly distinctive radiation pattern. Isolation might be enhanced by using EBG (electromagnetic band gap) based AMC (Artificial Magnetic conductor).

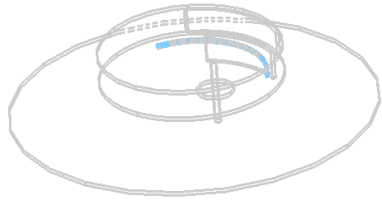
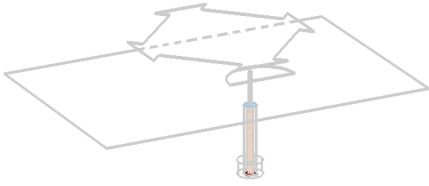
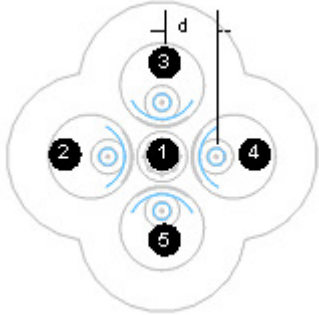
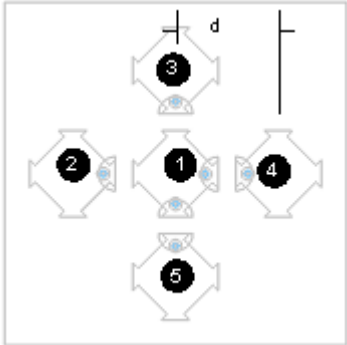


**Figure 2.17: Alternative Single pole four through (SP4T) using four highly decoupled corner antennas**

The SPA slot antenna is only one example of what can be achieved as reconfigurable antenna. Other antennas than slot could be used, taking into account the geometry of the navigation device, with different radiation characteristics in terms of pattern or polarization.

Table 2.1 shows two MEMtenna unit cells using miniature antennas, which are different from the canonical slots or wire antennas presented before.

**Table 2.1: Dual axis SPA reconfigurable antenna using DIME or PP miniature antenna**

	DIME Antenna [DA]	Coupled pentagonal patch [PP]
Basic Radiator		
MEMtenna unit cell Geometry		

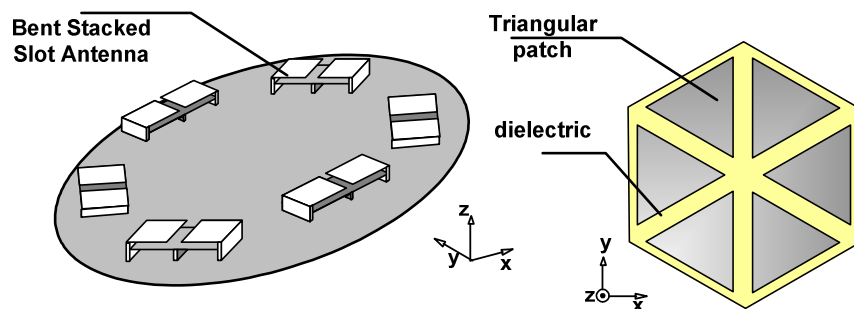


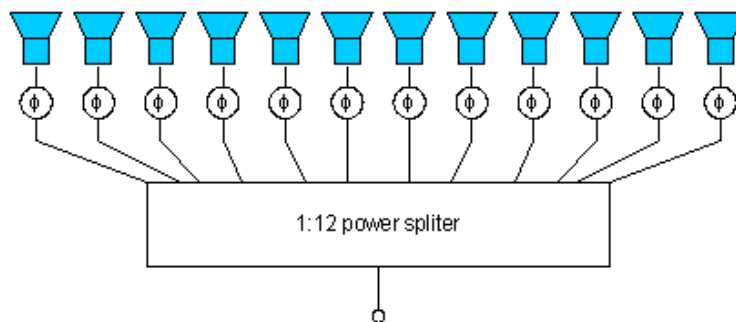
**Figure 2.18: Variant of Electronically Steerable Passive Array Radiator (ESPAR) antennas**

We investigated higher degrees of reconfigurability in terms of radiation pattern, polarization, and input impedance. This SPA (mono or multi axis) can be deployed alone (smaller form factor) or in arrays of SPA cells.  $N \times N$  arrays could be deployed. As the parasitic elements are not active, the spacing requirement will be applied only to the central active RF elements, but not necessarily to the other (passive) elements.

For instance a  $3 \times 3$  array could be deployed on a laptop (35x35cm form factor), while a  $2 \times 2$  (23x23 cm) or  $2 \times 2 \times 1$  could be deployed on a miniPC.

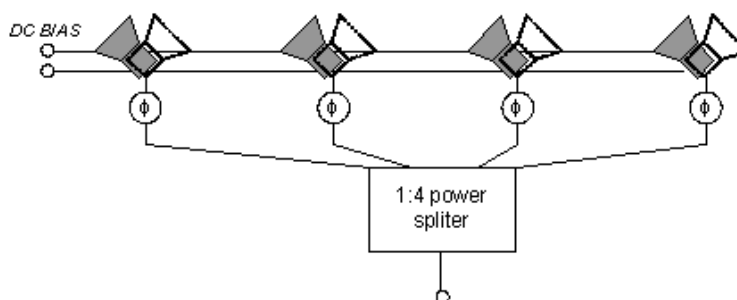
Regarding the GRABEL PoC form factor of  $5 \times 5 \lambda/2$  spaced elements, which reach 500x500mm, we could envisage to have a  $4 \times 4$  or  $5 \times 5$  elements. Let us recall here the principle of the networks to phased array. Such an array, as that presented on

figure 2.19 consist of several elementary antenna elements spaced by a distance  $d$ . The output of each element goes through an amplitude ( $a_n$ ) and phase ( $\phi_n$ ) weighting before being summed up in a power combiner. In the canonical case of a linear phased array, each amplitude  $a_n$  is identical and according to the Direction-of-Arrival angle  $\theta_{DOA}$  aimed at the law of phase is written as  $\phi_N = -2\pi \cdot d \cdot \sin(\theta_{DOA})$ . The electromagnetic field is simply expressed using the superposition law of phase of the linear systems:  $E_{array}(\theta, \phi) = E_{cell} \times AF$  where  $E_{cell}$  is the field of an elementary source or cell and AF is the array factor. Directivity can thus be increased by using cells which are already forming a beam in a privileged direction.



**Figure 2.19: "Classical" Phased array using twelve elementary sources.**

In order to limit the number of antenna elements, one can use DC-controlled reconfigurable cells as in the scheme presented on figure 2.20. The advantages of such an architecture are multiples. For directivity and a comparable capacity of reconfigurability, the size of the network is brought back to a tiny size which allows an easier integration in the modern systems.



**Figure 2.20: "Array using four reconfigurable cells having each a reconfigurability capacity for a global similar directivity.**

Thus 4 phase-converters are necessary (instead of 12) and a 1:4 power divider is from now on sufficient whereas in its traditional version the RF circuit is much more complex. This simplification results in a greater tolerance of the complete network compared to the precision of realization and a reduction of cost for industry involved. Especially the losses in the RF lines, which can be very important for such complex networks, are much reduced here. This consequently guarantees better levels of radiation.

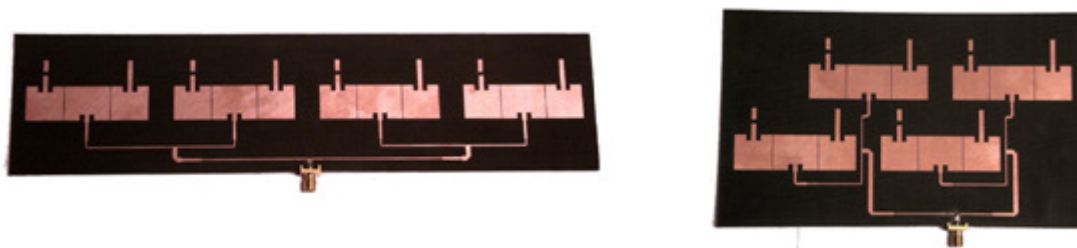


**Figure 2.21: Inline and quincunxes WLAN arrays of SPAs**

The principle of the reconfigurable antenna containing MEMS RF can thus be extended to other types of aerial elements like patches, and make it possible to carry out arrangements of reconfigurable cells as that is presented on figure 2.23.

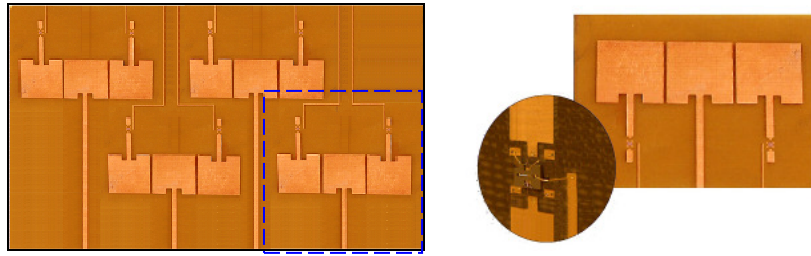


**Figure 2.22: "Adaptive antenna based on four reconfigurable cells (a) and reconfigurable cell using patch as radiating elements (b).**

The simulated radiation pattern of a network of 4 simple patches ( $d=\lambda_0$ ) to which one affects a linear law of phase to make it point towards  $\theta_{DOA}=35^\circ$ . The peak gain of the antenna array (in the direction of the main lobe ( $\theta_{AL}=-35^\circ$ )) is 11dBi. By increasing the number of patch to 12 as in the configuration of

figure 2.19, the peak reaches 22dBi in the direction  $\theta_{DOA}$ . The ripples observed in the radiation pattern are very important and the back lobe remains very important. In addition this configuration imposes a size of network of  $L=12 \lambda_0$ . On the other hand by employing a reconfigurable array with 4 cells (as in figure 2.20) roughly the same gain achieved by a 12 cell array is obtained. Beyond the profit in term of integration and simplicity of RF circuit, the back lobe is reduced in a drastic way. This technique makes it possible to form good beams for modern telecommunications systems.

The GNSS Reconfigurable Antenna based Enhanced Localization (GRABEL) is from CSEM PoV the use of any (miniature) reconfigurable antenna solution, with polarization and/or radiation pattern diversity.

The full validation (PoC GRABEL system) will open the door for a new system and antenna design approach that will ultimately be used, after the project, by GRABEL SMEs, in order to address GNSS localization through the use of baseband and reconfigurable antenna technologies combination. The process will be used for the PoC system and extended to the other use cases:

- Application, use case identification
- Propagation Environment
- Derivation of form factor, rough sketch geometry estimated
- Derivation of achievable radiation pattern and/or polarization agility, DoF, and number of active (reconfigurable) antenna elements/cells used. Depending on the application, form factor, and industrial or cost constraints Reconfigurable antenna and beamforming baseband technique might be replace by non-reconfigurable antenna and diversity/combining techniques
- Design and integration of (reconfigurable) antenna solution and associated feed networks, or combining /diversity circuits
- Development of baseband and beamforming algorithm.

The GRABEL proof-of-concept system is in CSEM PoV that, given the important size of the antenna array, only high performance applications that can cope with such big antenna arrays can be envisaged. Geodesy, mapping or alternatively logistics are possible examples. Logistic application could be for instance pallets transportation in a semi-open hangar, or precise container localization on a harbor, or emergency vehicle localization in urban area. As the latter emergency vehicle has to be precisely localized when stopped; Inertial MEMS unit GPS aiding is useless. Please note that such a car roof mounted antenna system for enhanced localization in urban area or light indoor, has been identified as being a high potential application for GRABEL system exploitation.



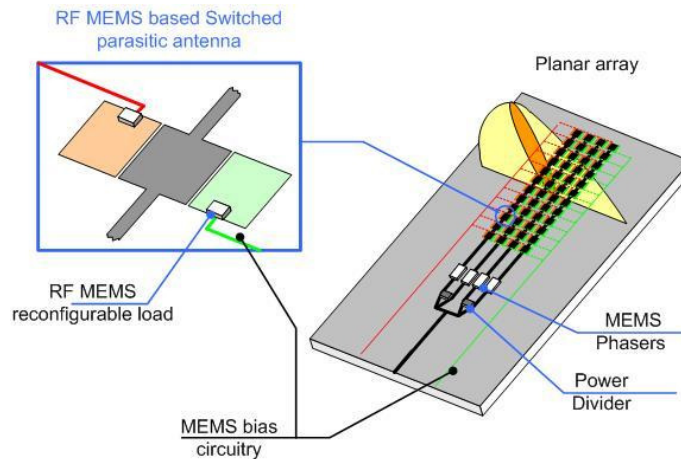


Figure 2.23: RF MEMS based beamforming array [Peti07]

### 2.2.5 Discussion on SPA padding in arrays

In its simpler version, the SPA-2 using only two parasitic antennas can achieve four different radiation patterns by using appropriate loading of the latter parasitic antenna. The parasitic antenna can notch the radiation pattern or generate some diversity. The different radiation patterns that are achievable with such parasitic antenna are presented in figure 2.24.

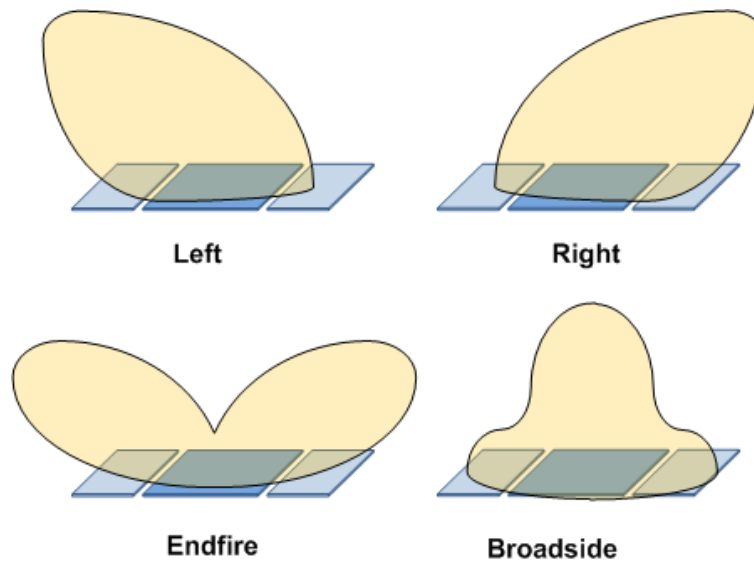
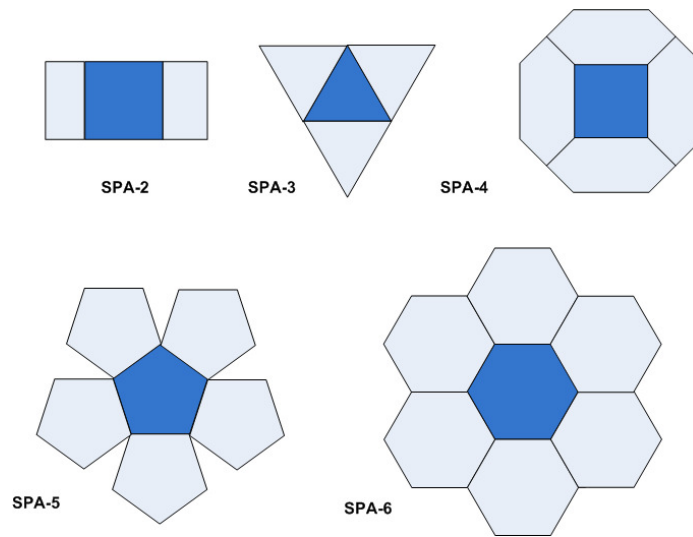


Figure 2.24: Achievable radiation pattern with two elements switched parasitic antenna (SPA-2)

The SPA concept can be extended to N axes. Figure 2.25 presents a different order of SPA, from the afore mentioned one. At GPS-L1 frequency, the overall size of this SPA “unit cell” is dependant of the shape, but regardless of the SPA’s order, the maximum length can be brought down to  $2 \times \lambda/3$ . AT GPS-L1 frequency, that’s 12-15cm.



**Figure 2.25: Different order of SPA from SPA-2 to SPA-6**

Using this SPA-N as unit cell of a padding, we envision to associate a set of this unit cells in a specific surface. For instance figure 2.26 presents the padding of 4 SPA and a central active element, while figure 2.27 presents the assembly of SPA-4 in a 4, 5 or 7 elements configuration.

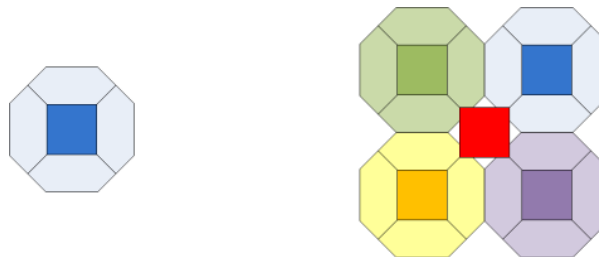


**Figure 2.26: Assembly of SPA-4 in 5 active elements array (overall dimension 30x30cm)**

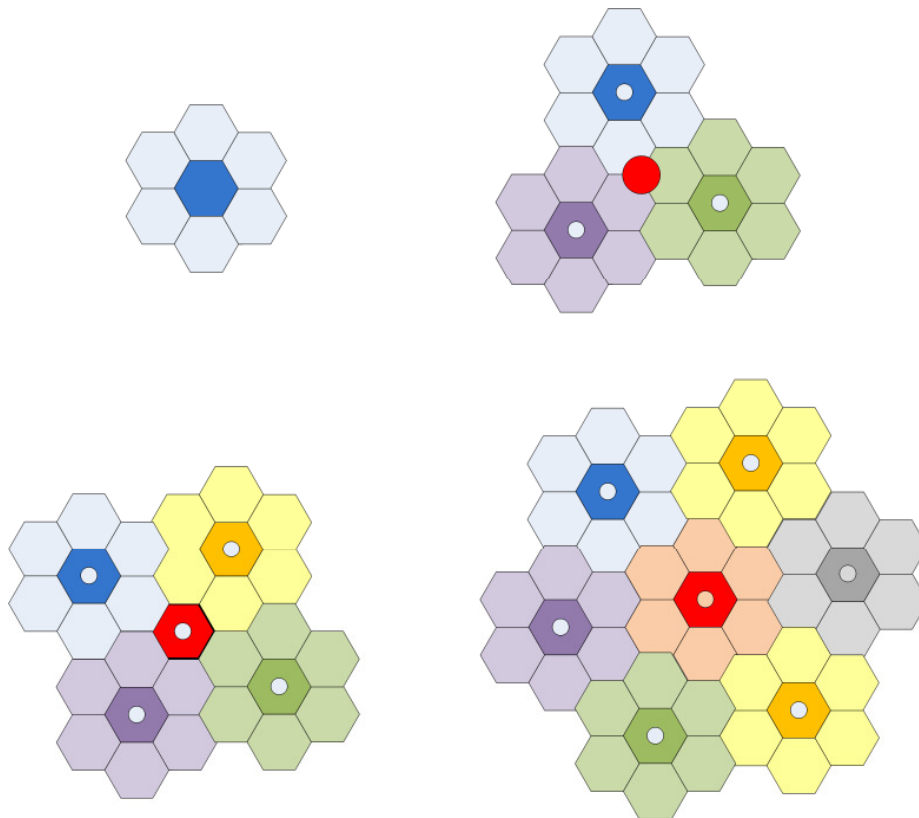


**Figure 2.27: Assembly of 1 SPA-6 in 4-5-7 active elements array (larger dimension are respectively 15-30-37-45 cm)**

Within GRABEL, we envision also comparing the classical way of designing and using  $\lambda/2$  spaced “isotropic” source with the equivalent sized array with parasitic antenna interleaving. Indeed, another way to see MEMtenna array instead of classical array design is to consider that we are using the spare place between active element in order to get better radiation pattern or polarization agility.

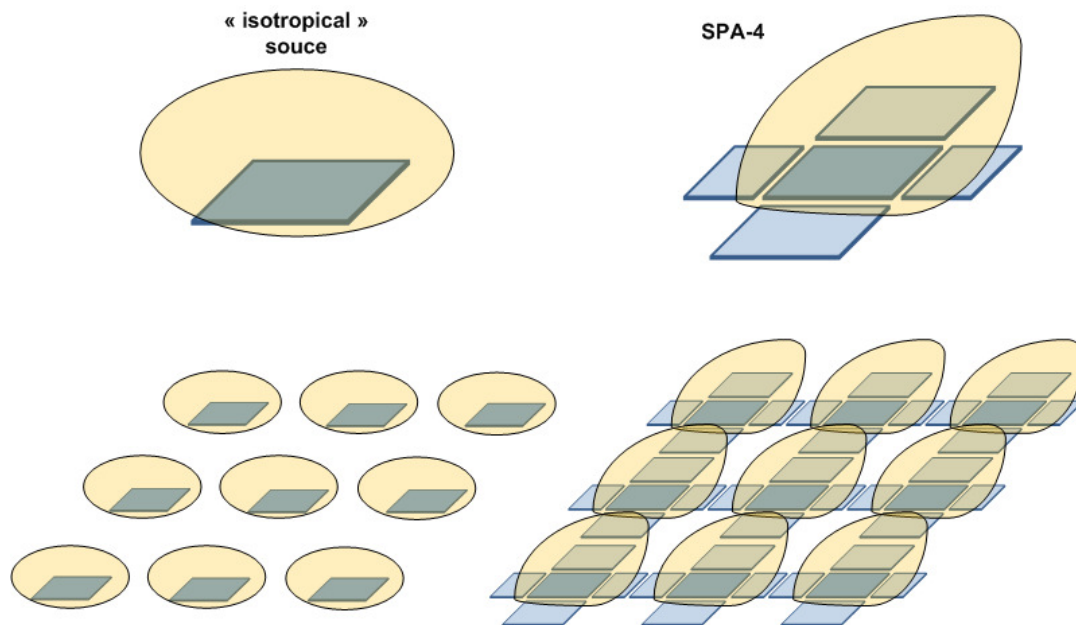


**Figure 2.28: 3x3 array using classical “isotropical” sources and SPA-4 array equivalent to parasitic antenna element interleaving**

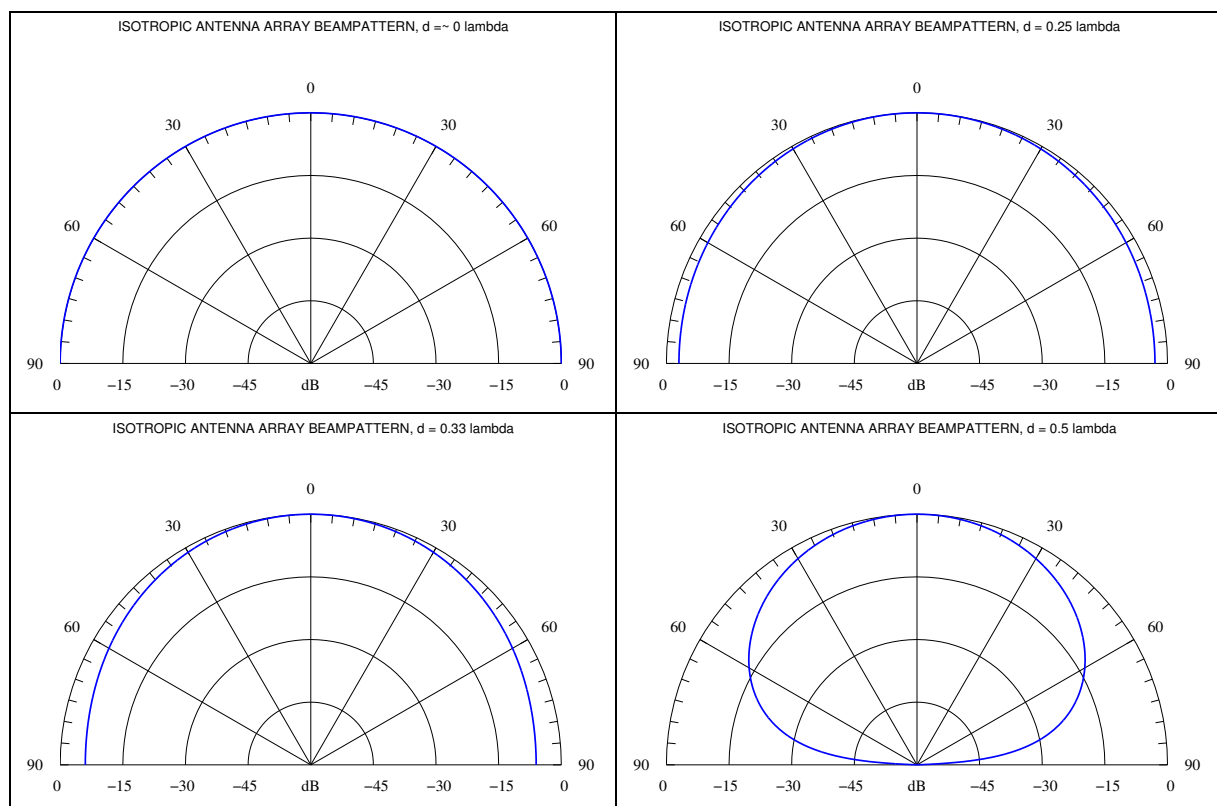
### 2.2.6 Determining the antenna's distance in the array

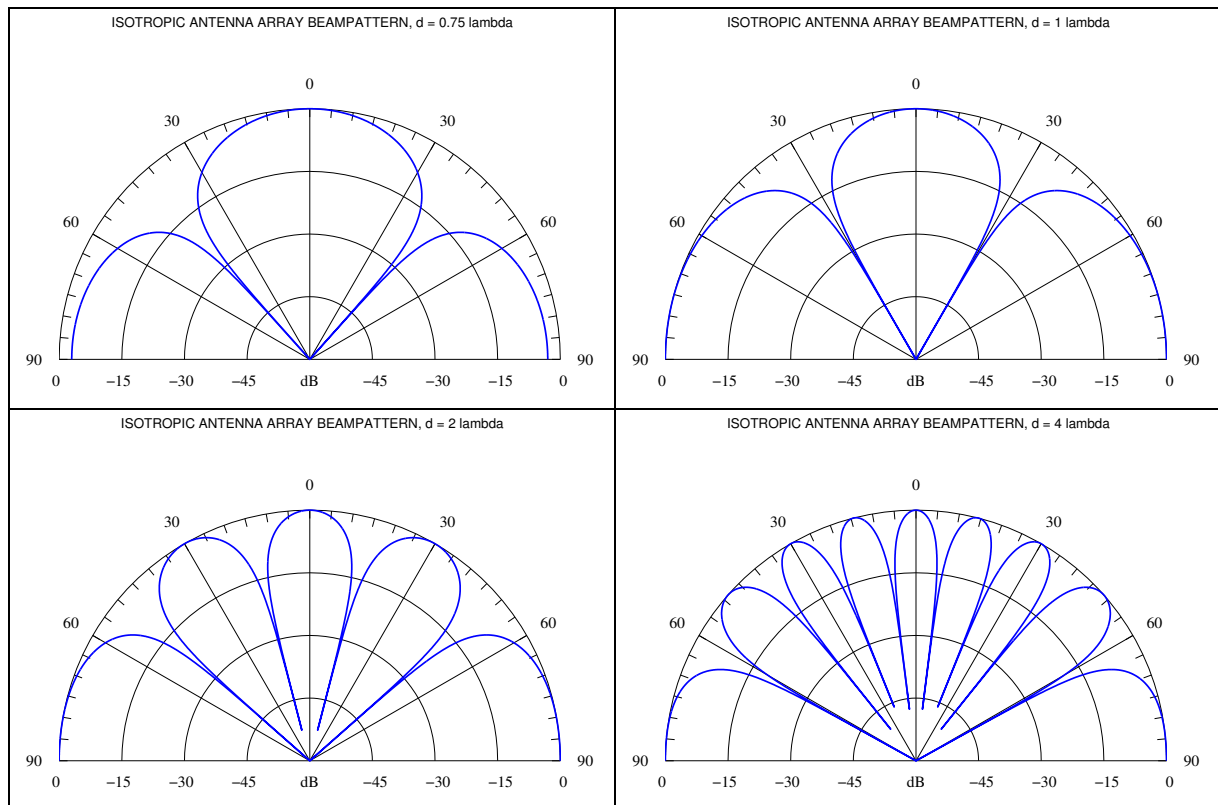
The board dimensions are directly determined by the GNSS signal's frequency; in our case we are interested in the L1 and L5 band of GPS. The distance between the antennas ideally should be  $\lambda/2$ , therefore  $4(\lambda/2)+l$  is the minimal dimension of the board (where  $l$  is the length of a antenna). As reminder GPS-L1 wavelength is 190mm. Spacing's below  $\lambda/2$  produce a large lobe, thus have a poor beamforming capability. Larger spacing's, above  $\lambda/2$ , result in large lobes at low elevation (where most interference and multipath comes from) and are therefore also unfavorable. Distances around  $\lambda/2$  can be considered good solutions giving a sufficiently sharp main lobe without excessive low elevation side lobes. (-6dB at  $\pm 41.7^\circ$ ).

The simulations presented hereafter were conducted as a starting point for further analysis and algorithm preparation and for the specification upon the distance between antennas in the frame of the GRABEL project.

First of all, table 2.2 **Error! Reference source not found.** shows the radiation pattern of a 2 isotropic antenna array, pointing at 0 degrees. Distances equal or higher to  $\lambda = 1$  result in a thin lobe pointing at the desired signal with relatively big side lobes. Decreasing  $\lambda$  the side lobes became smaller, meanwhile the main lobe increases in size. At  $\lambda/2$  and smaller distance the side lobes aren't present anymore and the main lobe increases in size tending to form one unique isotropic antenna radiation pattern.

**Table 2.2: 2 antenna isotropic beam patterns ( $d = 0 - 4\lambda$ )**





The targeted signals in the frame of the GRABEL project are L1 and L5, so the distance choice must be focused to optimize these signals. Table 2.3 **Error! Reference source not found.** shows the GNSS signal bands for GPS III, Galileo, Glonass and Compass/Beidou-2 systems.

**Table 2.3: Table of GNSS frequencies**

Frequency band	Frequency $f$ [MHz]	Wavelength $\lambda$ [m]	$\lambda/2$ [m]	$\lambda/2$ [mm]
<b>GPS</b>				
<b>L1</b>	1575.42	0.19029	0.09514	<b>95.14</b>
<b>L2</b>	1227.60	0.24421	0.12210	<b>122.10</b>
<b>L5</b>	1176.45	0.25482	0.12740	<b>127.40</b>
<b>E5a</b>	1164	0.25755	0.12876	<b>128.76</b>
<b>E5b</b>	1215	0.24674	0.12336	<b>123.36</b>
<b>E6</b>	1278.75	0.23444	0.11722	<b>117.22</b>
<b>E2-L1-E1</b>	1559 - 1592	0.19230 - 0.18831	0.09614 - 0.09416	<b>96.14 - 94.16</b>
<b>Glonass</b>				
<b>L3</b>	1207,140	0.24835	0.12418	<b>124.18</b>
<b>Compass</b>				
<b>E2</b>	1561.10	0.19204	0.09602	<b>96.02</b>
<b>E1</b>	1589.74	0.18858	0.09428	<b>94.28</b>
<b>E6</b>	1268.52	0.23633	0.11816	<b>118.16</b>
<b>E5b</b>	<b>1207.14</b>	<b>0.24835</b>	<b>0.12418</b>	<b>124.18</b>

Example of distance between antennas depending on the targeted frequency band:

$$f_{L1} = 1575.42\text{MHz}, \quad \lambda = 0,19029\text{m} \quad \Rightarrow \quad \lambda / 2 = 0.09515\text{m}$$

At  $0.5\lambda_{L1}$  a 9 antenna cross array would measure on each side approximately 0.43 meters.

Taking in consideration the L1 and L5 frequencies and searching for a possible solution in terms of dimension & quality compromise the following distance can be proposed:

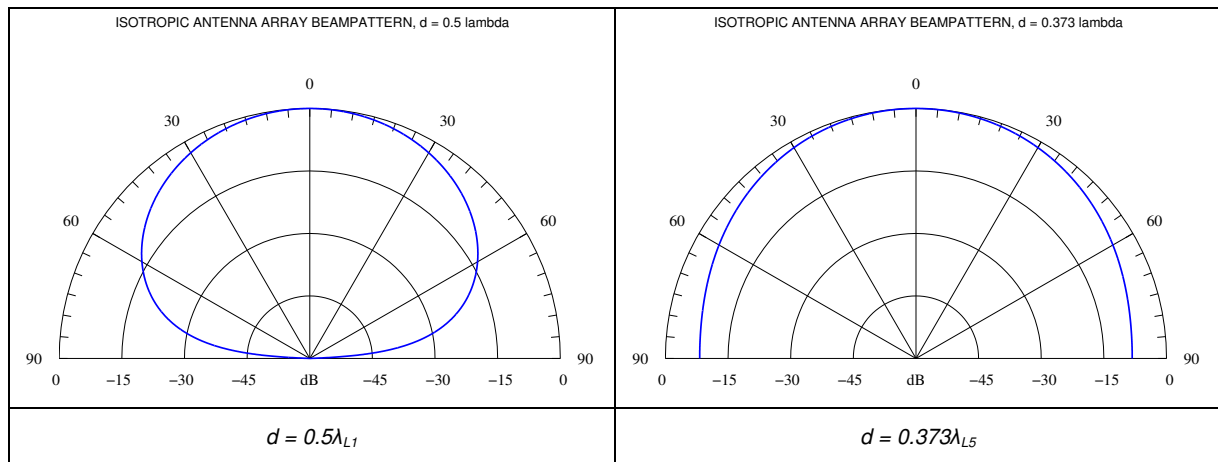
$$f_{L1} = 1575.42\text{MHz}, \quad \lambda = 0,19029\text{m} \quad \Rightarrow \quad 0.5\lambda_{L1} = 0.09515\text{m}$$

$$f_{L5} = 1176.45\text{MHz}, \quad \lambda = 0,25482\text{m} \quad \Rightarrow \quad 0.5\lambda_{L5} = 0.12741\text{m}$$

Taking  $0.5\lambda_{L1}$  as compromise optimum one can see that  $0.5\lambda_{L1} = 0.373 \lambda_{L5}$ . So for L5 this can't be considered an optimal choice; For L1 the beam pattern is very promising, there aren't any side lobes and the horizontal gain is extremely low, so the antenna array won't be affected by horizontal interference and the main lobe shape has a gain of -6 dB at  $\pm 41.7^\circ$ . With a distance of  $0.373\lambda_{L5}$  the horizontal interference (gain = -8.2 dB at  $\pm 90^\circ$ ) will have a consistent influence on the L5 signals captured by the antenna array, in this condition no beamforming is possible.

Table 2.4 **Error! Reference source not found.** shows a comparison between the beam patterns for the 2 signal characteristics with the above mentioned distance configuration

**Table 2.4: 2 antenna isotropic beam patterns ( $d = 0.09515\text{m}$ )**



A better compromise that fits both signal frequencies can be calculated with the geometric mean between the two wavelengths  $\sqrt{\lambda_{L1} * \lambda_{L5}}$ . The distance then will be:

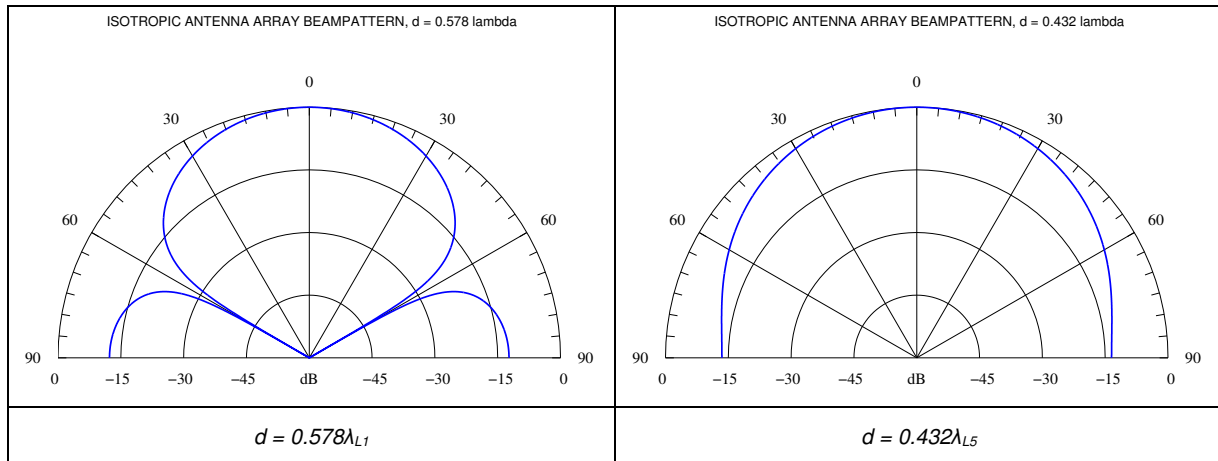
$$\lambda = 0.22020\text{m}$$

$$d = \lambda / 2 = 0.578\lambda_{L1} = 0.432\lambda_{L5}$$

With this distance configuration  $\lambda_{L1}$  has a gain of -6dB at  $\pm 35.1^\circ$  while  $\lambda_{L5}$  has a gain of -6dB at  $\pm 50.4^\circ$ . The horizontal side lobe for the L1 signal has a gain of -12.3 dB at  $\pm 90^\circ$ , while for L5 the horizontal gain is -13.4 dB at  $\pm 90^\circ$ .

**Error! Reference source not found.** Table 2.5 shows the isotropic beam patterns for a 2 antenna system with the calculated distance.

**Table 2.5: 2 antenna isotropic beam patterns ( $d = 0,11010m$ )**



Considering that in the frame of the GRABEL project the first targeted signal will be L1 the final decision was to use  $d = 0.5 \lambda_{L1} = 0.09515 \text{ meters}$  as distance between the antennas in the array.

### 2.2.7 Placement and number of antennas – spatial configuration

This chapter presents a study upon spatial configuration, symmetry & shape, mutual influence between the antenna array’s antennas. The study starts at HW level and leads towards the specific mutual influence aspects, beam directivity, beam sharpness and complexity of the resulting numerical computation.

The possible configurations of the multichannel RX board can be resumed as follows:

- Single antenna
- Inline array of antennas
- Square array of antennas
- Crossing arrays
- Triangular and hexagonal configuration

Complete 5x5 or 4x4 quadratic array configurations will not be studied since emphasis is set on testing some relevant configurations that come out of this study.

There is a number of mutual influence parameters depending on the number of antennas and shape of the configuration. These parameters are represented in a symmetric matrix; the symmetry exists because the influence of a antenna towards another is the same in both directions. All the parameters are linearly dependent; several of them are redundant in the matrices because of equal distance.

The possible distances between single antennas are:  $nx, nx\sqrt{2}, x\sqrt{3}, nx\sqrt{5}, x\sqrt{10}, x\sqrt{13}, x\sqrt{17}$ . Where  $x$  is the minimal distance i.e.  $\lambda/2$  and  $n$  is a multiple.

Some of the above mentioned lengths are very close, so eventually, from a practical/computational point of view, they will be considered as a single parameter. Some other parameters will eventually be removed due to lack of influence on the beamforming performance.

Table 2.6 resumes the key points of the antenna configuration study.

**Table 2.6: Key points of antenna configuration study**

CRITERIA	EFFECTS
<b>Symmetry</b>	The more an array has a symmetrical shape, the greater is the beam flexibility. To enhance beam steering precision towards specific areas one can use less symmetrical configurations, although this should be used only in specific situations.
<b>Number of antennas</b>	The more antennas are present on a linear array, the bigger is the primary to secondary beam ratio. Along the linear array a high precision of beam steering can be reached. The more antennas are present in the configuration, the more computational power is required.
<b>Mutual influence parameters</b>	Different parameters enhance theoretical precision. On the practical side they enhance computation and don't necessarily enhance beam directivity and signal reception accuracy.
<b>Distances between antennas and configuration shape</b>	Distance between antennas determinates how the signals will be summed. The choice of the distance between antennas in 3D beamforming is strictly connected to the configuration shape.

In the following pages some of the possible spatial configurations are presented and described considering the upon mentioned criteria. The best promising configurations will then be analyzed and simulated.

### 2.2.7.1 Single antenna

**Table 2.7: Single antenna**

**a.1 1 antenna:** 1 element matrix, 1 parameter.

No beamforming is possible with this configuration.



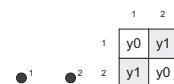
### 2.2.7.2 Inline array of antennas

Inline array antennas have an axial symmetry and can so direct the main lobe only on one line (2D Beamforming).

**Table 2.8: Inline array of antennas**

**b.1 2 antennas linear array:** 2x2 matrix with 2 parameters.

$y_0$  is the parameter of auto influence, which is the same for both antennas,  $y_1$  is the mutual influence between the antennas.



**b.2 3 antennas linear array:** 3x3 matrix, 3 parameters.

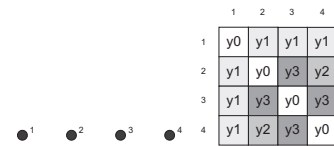
The mutual influence between 1-2 and 2-3 is the same, therefore  $y_1$  is used to describe both mutual influences.





**b.3 4 antennas linear array:** 4x4 matrix, 4 parameters.

This configuration enables a better main beam steering compared to the previous ones.



These considerations can be extended to n-antenna arrays. The system complexity increases linearly.

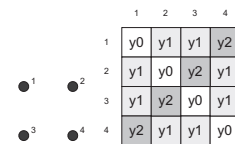
2.2.7.3 Antennas disposed in a square

**Table 2.9: Antennas disposed in a square**

**c.1 4 antennas square array:**

4x4 matrix, 3 parameters.

This configuration has a better symmetry compared to linear arrays, allows 3D beamforming and has few parameters.

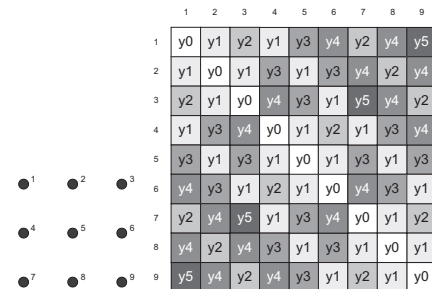


**c.1 9 antennas square array:**

9x9 matrix, 6 parameters.

Very symmetrical configuration with great beam flexibility.

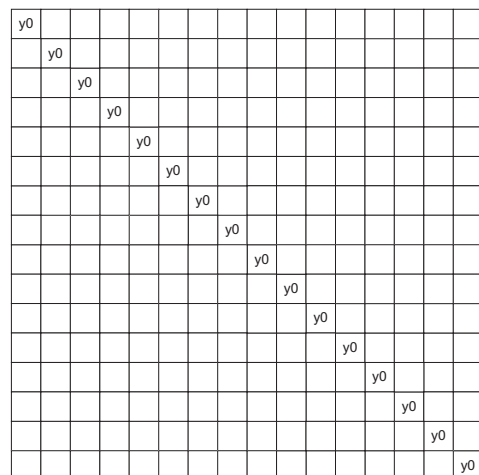
Computation power is high.



**c.3 16 antennas square array:**

16x16 matrix, 10 parameters.

Computation power is very high.



These considerations can be extended to n-antenna square arrays. There is a quadratic complexity increase when referring to the square dimension increase.

### 2.2.7.4 2 crossing arrays

**Table 2.10: 2 crossing antenna array**

#### d.1 9 antennas L shape array:

9x9 matrix, 15 parameters.

This configuration has the same number of parameters as the 25 antennas square array, but with only 9 antennas.

This configuration can reach a high precision in beam steering towards the inner L region.



	1	2	3	4	5	6	7	8	9
1	y0	y1	y2	y3	y4	y11	y13	y14	y8
2	y1	y0	y1	y2	y3	y10	y12	y7	y14
3	y2	y1	y0	y1	y2	y9	y6	y12	y13
4	y3	y2	y1	y0	y1	y5	y9	y10	y11
5	y4	y3	y2	y1	y0	y1	y2	y3	y4
6	y11	y10	y9	y8	y1	y0	y1	y2	y3
7	y13	y12	y6	y9	y2	y1	y0	y1	y2
8	y14	y7	y12	y10	y3	y2	y1	y0	y1
9	y8	y14	y13	y11	y4	y3	y2	y1	y0

#### d.2 9 antennas L-cross shape array:

9x9 matrix, 11 parameters.

Similar characteristics as in the L configuration.



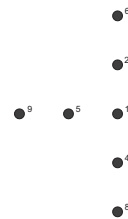
	1	2	3	4	5	6	7	8	9
1	y0								
2		y0							
3			y0						
4				y0					
5					y0				
6						y0			
7							y0		
8								y0	
9									y0

#### d.3 9 antennas cross shape array:

9x9 matrix, 8 parameters.

Moving from an L to a cross configuration the symmetry raises, and the number of parameters decreases.

This is a particular configuration because most of the parameters are multiples of each other.



	1	2	3	4	5	6	7	8	9
1	y0	y1	y1	y1	y1	y2	y2	y2	y2
2	y1	y0	y5	y2	y5	y1	y7	y3	y7
3	y1	y5	y0	y5	y2	y7	y1	y7	y3
4	y1	y2	y5	y0	y5	y3	y7	y1	y7
5	y1	y5	y2	y5	y0	y7	y3	y7	y1
6	y2	y1	y7	y3	y7	y0	y6	y4	y6
7	y2	y7	y1	y7	y3	y6	y0	y6	y4
8	y2	y3	y7	y1	y7	y4	y6	y0	y6
9	y2	y7	y3	y7	y1	y6	y4	y6	y0

#### d.4 9 antennas T-cross shape array:

9x9 matrix, 10 parameters.

This and the following configuration can reach a good beam steering towards the bottom region.



	1	2	3	4	5	6	7	8	9
1	y0								
2		y0							
3			y0						
4				y0					
5					y0				
6						y0			
7							y0		
8								y0	
9									y0

#### d.5 9 antennas T shape array:

9x9 matrix, 12 parameters.

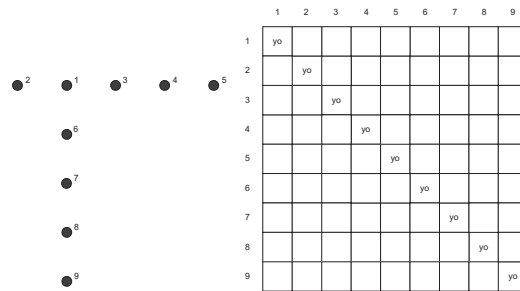
The T shape, similar to the L shape, has a big number of parameters.



	1	2	3	4	5	6	7	8	9
1	y0								
2		y0							
3			y0						
4				y0					
5					y0				
6						y0			
7							y0		
8								y0	
9									y0

**d.6 9 antennas LT shape array:**

9x9 matrix, 9 parameters.



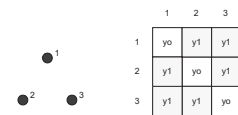
2.2.7.5 Triangular and hexagonal configuration

**Table 2.11: Triangular and hexagonal configuration**

**e.1 3 antennas triangular shape array:**

3x3 matrix, 2 parameters.

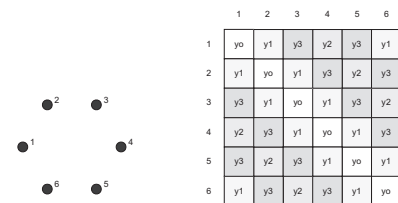
Very simple symmetrical configuration.



**e.2 6 antennas hexagonal shape array:**

6x6 matrix, 4 parameters.

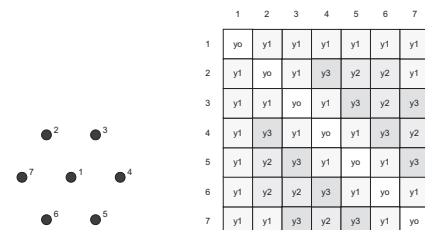
Highly symmetrical configuration with good beam steering capabilities. Eventually not suited for horizontal tracking.



**e.3 7 antennas hexagonal shape array:**

7x7 matrix, 4 parameters.

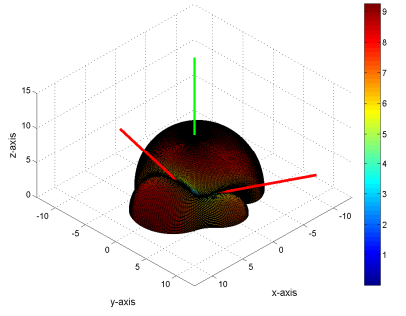
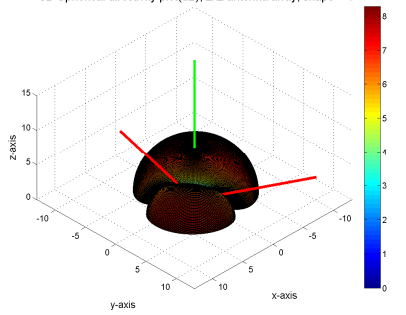
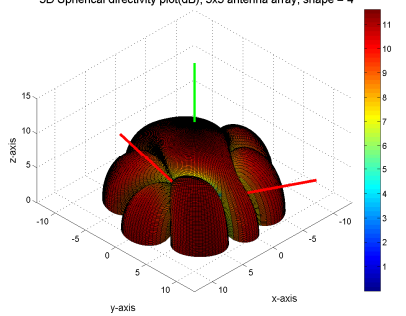
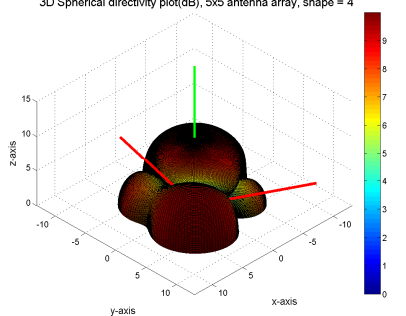
This configuration should improve a little the beam steering capabilities of the previous one.



Some beamforming simulations with LCMV were done to do a first investigation on the effects of the different number of antennas and configuration. Table 2.12 shows some 3D simulation results of various antenna array configurations. In this case the simulation's intent is to steer one signal and mitigate two interferers, normally for the GRABEL solution the main goal will be to steer about 4 satellites signals and mitigate eventually 1 interferer, if any. For every simulation the signal (green) and interferer (red) position is the same. It is clear that a 4 antenna isn't able to fully handle 3 signals, but as one can see is to solve the mitigation problem by putting both interferers' DOA in the same plane and mitigating that interference plane. The 9 antenna cross array deals with the problem with higher precision, the lobe steering the signal is thinner and also the accuracy of mitigation is higher. Obviously in the 9 antennas cross array antenna there are some more side lobes, they will normally be used to steer signals.

Another consideration is the higher precision of steering when the distance between the antennas is  $1/2\lambda$ .

**Table 2.12: 3D simulation of 2x2 square and 9 antennas cross configurations**

<p>2x2 square (4 antennas) d= 1/2λ</p>	<p>3D Spherical directivity plot(dB), 2x2 antenna array, shape = 1</p> 
<p>2x2 square (4 antennas) d= 1/4λ</p>	<p>3D Spherical directivity plot(dB), 2x2 antenna array, shape = 1</p> 
<p>9 antennas cross d= 1/2λ</p>	<p>3D Spherical directivity plot(dB), 5x5 antenna array, shape = 4</p> 
<p>9 antennas cross d= 1/4λ</p>	<p>3D Spherical directivity plot(dB), 5x5 antenna array, shape = 4</p> 

### 2.2.8 Results and candidate selection

Taking into account the following tables and results it is possible to see that there are some shapes that are more suitable for an optimal performance.

Table 2.13 shows a comparison of linear, L and square configurations in relation to the dimension (antennas) and parameter number.

**Table 2.13: Spatial configuration vs. number of parameters**

Dimension	Shape							
	Linear		L		X		Square	
Maximal Extension	antennas	parameters	antennas	parameters	antennas	parameters	antennas	parameters
2x2	2	2	3	3	4	3	4	3
3x3	3	3	5	6	5 4	4 3	9	6
4x4	4	4	7	10	8	7	16	10
5x5	5	5	9	15	9 8	8 7	25	15
NxN	N	N	2N-1	$N(N+1)/2$	2N 2N-1 2N-2	2N-1 2N-2 2N-3	$N^2$	$N(N+1)/2$

Table 2.13 summarizes some of the already showed configurations and expresses in arithmetic sizes. The linear case is quite predictable and simple, it doesn't need particular comments. The comparison between L and square configurations shows interesting aspects; as far as the dimension increases the number of parameters for both shapes increases equally, nevertheless square configurations are symmetrical, therefore both type of configurations have own application fields.

The number of antennas increases drastically in the square configurations, so the general complexity increases too. The consequences of this are high material costs, impossibility to handle big dimension numbers due to the great amount of signals at DSP input, data quantity to process and also mutual admittance matrix complexity.

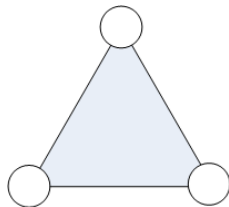
At this point it is questionable what type of configuration is the most suitable in relation to number of antennas. Table 2.14 shows some of the possible configurations. As we can see some L type configurations are very suited for a high parameter resolution, clearly not all of them are suited for our 5x5 matrix board. Square and cross and hexagonal configurations have a great symmetry advantage, which reduces parameters.

**Table 2.14: Number of antennas vs. matrix complexity and parameters**

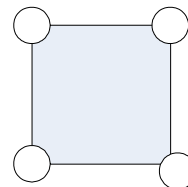
N° Antennas	Configuration Type	Matrix Complexity	Parameters
1	monopole	1	1
2	array	4 (2x2)	2
3	array	9 (3x3)	2
3	triangle	9 (3x3)	2
4	2x2 square	16 (4x4)	3
4	array	16 (4x4)	4
5	X	25 (5x5)	4
5	array	25 (5x5)	5
6	6 antenna hexagon	36 (7x7)	4
7	7 antenna hexagon	49 (6x6)	4
9	3x3 square	81 (9x9)	6
9	X	81 (9x9)	8
9	T	81 (9x9)	12
9	L	81 (9x9)	15

Finally table 2.15 presents the configurations chosen as best candidates for further testing.

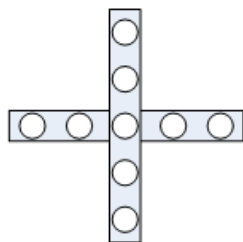
**Table 2.15: Best candidate antenna arrangement retained for further testing**



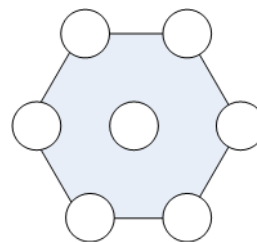
**3 receivers triangle antenna array**



**4 receivers square antenna array**



**5/9 receivers cross antenna array**



**6/7 receivers hexagonal antenna array**

### 2.2.9 GRABEL antenna system

The studied system is a square shaped board that can host single front-end channel receivers. The board has 25 slots aligned in a 5x5 rectangular matrix, 4 more slots are provided to configure a hexagonal array shape. The main goal is to be able to interface as many receivers as needed, connecting them in the desired spatial configuration.

The board's output should be a set of digitized signals depending on the number of implemented single front-end channel receivers. The following image shows a general system block diagram:

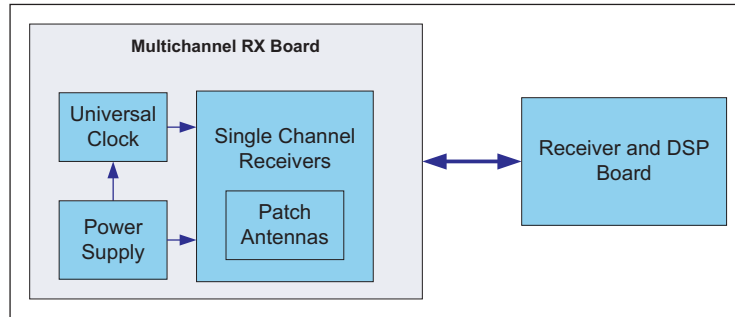


Figure 2.29: General system block diagram

Figure 2.30 represents such a multichannel RX board with all the mentioned configurations (right), and with only the best promising configurations (left).

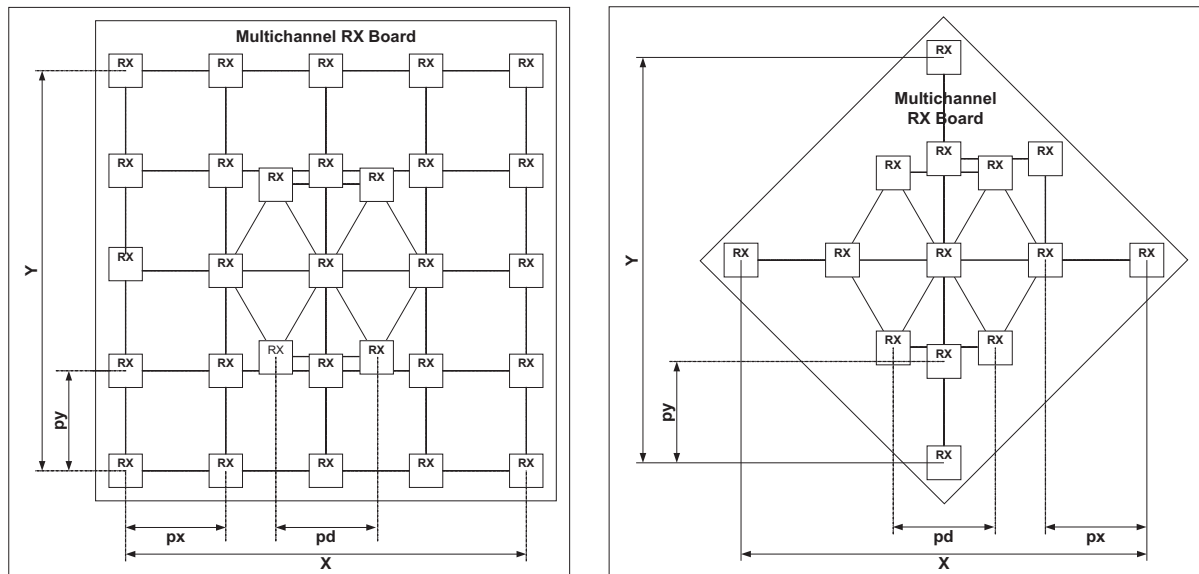


Figure 2.30: Complete antenna array (right), antenna array subset for the selected configurations (left)

Where:

- X and Y are the total array dimensions.
- px, py, pd are the distances between the antenna slots, they should all measure  $\lambda/2$ .

In order to estimate relevant board configurations in terms of beam directivity, precision and computational performance, a little theoretical study has been done. Efficiency of the configuration depends on several criteria like configuration symmetry, number of single front-end channel receivers and distance between them. Theoretical, simulated and practical results will show the best promising models to implement efficient beamforming techniques.

### 2.2.9.1 Array of MEMtennas

The latter switched parasitic elements are loaded with passive phase shifters that can consist of variable capacitance or switched capacitance bank. The full RAS system could also involve a RHCP/LHCP polarization switch. One may also consider polarization switch on the parasitic element themselves (see figure 2.31). Concerning the switching device, in the frame of the GRABEL project it has been decided to focus on the proof of concept of GNSS Reconfigurable antenna enhanced localization system by using solid state device in a first place because of the practical integration matter bias voltage handling. Indeed high voltage require additional voltage step up component.

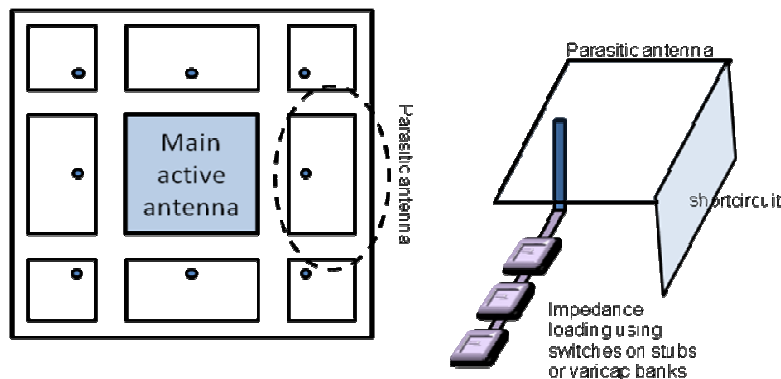


**Figure 2.31: SPA MEMtenna concept and detail of the parasitic antenna impedance loading**

RF-MEMS technology is not mature enough in summer 2009 to be involved in massive market devices such as those targeted by GRABEL SMEs. Apart from DelfMEMS which is still not available in a packaged version, they all require important power level which is brought by a secondary step-up converter. These devices are often developed for the ATE market (Automated Test Equipment for Semiconductors) and are still excessively expensive for the mass market that GRABEL SMEs are targeting. As a matter of fact, and regardless the high RF performances exhibited by the RFMEMS switching or variable capacitance devices, their solid state counterpart (e.g. MOS, GaAs, PIN) will be selected for the prototyping of GRABEL.

The latter mounting/ assembly/ control consideration on the Reconfigurable Antenna System should also take into consideration the possibility of combining antenna reconfiguration / diversity with multiple RF channels.

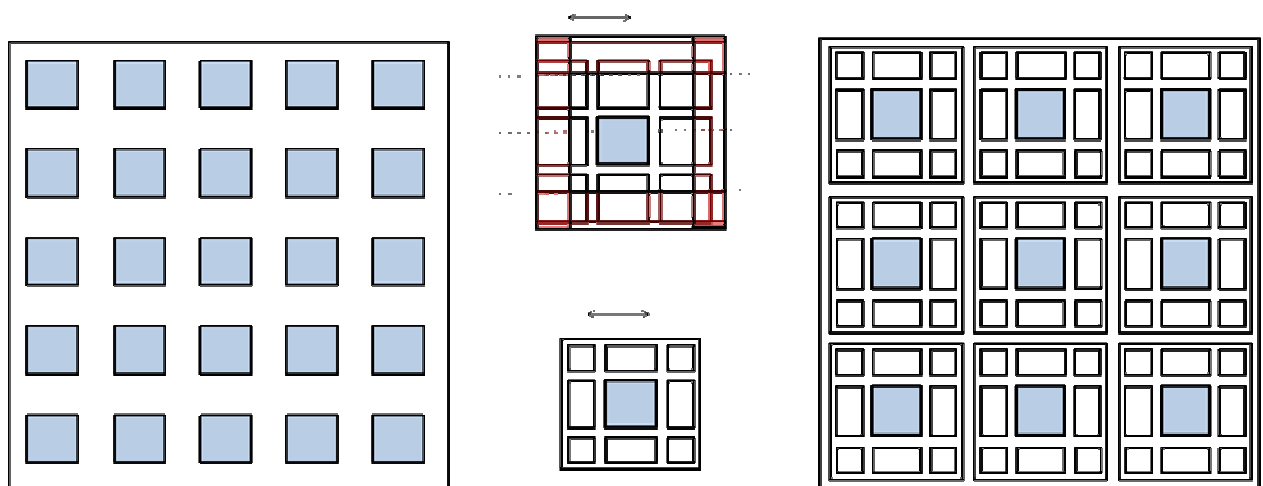




**Figure 2.32: 5x5 patch antenna array (left), MEMtenna unit cells (centre), achievable 3x3 MEMtenna array**

The PoC GRABEL antenna system will have the size of a 5x5 active antenna matrix. We will then consider mixing the 5X5 active patch antenna matrix with MEMtenna Switched Parasitic cells (figure 2.32). With the same size, we would then evaluate the integration of nine MEMtenna unit cells instead.

This consists of the combination of 9 radiation pattern agile sub-arrays in a 3x3 array.. The achievable beamforming will be less powerful than using a 25 element size matrix. But compared to this latter, the RF circuitry complexity and associated beamforming algorithm complexity would be then much simpler, along with the needed real time processing.

## 2.3 Architecture of the baseband processor

### 2.3.1 HW / SW partitioning

The receiver is a classical GPS receiver where the correlation engine is implemented in hardware and the rest of the processing is implemented in software.

The hardware collects all the signals coming from the front ends and performs all the classical operations associated to a classical GPS base band (Doppler removal, correlation, integration, dump).

The software does the rest of the operations like the tracking loops, the navigation message extraction, and the position fix computation. The beam forming management is another important task performed by the software. Basically the beam forming management code does not require a big integration within a classical GPS receiver. It can be added as a separate computational flow that needs some information from the GPS core and provide to the tracking engines the gain and phase corrections.

### 2.3.2 Beam forming or diversity

The process of standard beam forming doesn't exploit the possibility to steer the nulls of the antenna beam in the direction of the Radio Frequency Interferences (adaptive beam forming). These evolutions of standard beam formers are conceived to separate (analogically, digitally or both) a desired signal from one or more interfering signals (Spatial Filtering) by means of automatic and continuous characterization of the components of the weighting vector. This can be performed using a wide variety of different algorithms designed for many specific applications as reported in the table.

With these generic beam formers, the weighting vector  $\mathbf{W}$  is obtained using the signal  $\mathbf{x}(t)$  received by each receiver of the array (in some algorithms for special applications a reference signal is required).

Some of these will be probably tested in the Northern Cross SKA (*Square Kilometer Array*, <http://www.skatelescope.org/>) "test bed", in order to choose the more suitable one for either SKA or GNSS applications. If the adaptive algorithms are not based on a priori knowledge of the received signal (reference signal) but only based on a statistic information of the signal itself, as in the CMA (Constant Modulus Algorithm) and MV (Minimum Variance) algorithms, they are called **blind beamforming algorithms**.

**Table 2.16: Comparison of different beamforming algorithms [4]**

Algorithm	Optimization Criterion	Array Weight Solution	Comments
LCMV	$\min_{\mathbf{w}} \mathbf{w}^H \mathbf{R}_{xx} \mathbf{w}, \text{ s.t. } \mathbf{C}^H \mathbf{w} = \mathbf{f}^H$	$\mathbf{w} = \mathbf{f}^H \frac{\mathbf{R}_{xx}^{-1} \mathbf{C}}{\mathbf{C}^H \mathbf{R}_{xx}^{-1} \mathbf{C}}$	$\mathbf{C}$ contains constraint array response vectors. $\mathbf{f}$ is desired response values
GSC	$\min_{\mathbf{w}} [\mathbf{w}_o - \mathbf{C}_n \mathbf{w}]^H \mathbf{R}_{xx} [\mathbf{w}_o - \mathbf{C}_n \mathbf{w}]$	$\mathbf{w} = \mathbf{w}_o - \mathbf{C}_n \mathbf{w}_n,$ $\mathbf{w}_n = \frac{\mathbf{C}_n^H \mathbf{R}_{xx} \mathbf{w}_o}{\mathbf{C}_n^H \mathbf{R}_{xx} \mathbf{C}_n}$	$\mathbf{C}$ & $\mathbf{f}$ as in LCMV. $\mathbf{C}_n = \text{Null}\{\mathbf{C}\}$ . $\mathbf{w}_o = \mathbf{C}(\mathbf{C}^H \mathbf{C})^{-1} \mathbf{f}$ .
MSC	$\min_{\mathbf{w}_a} E\{ \mathbf{x}_m - \mathbf{W}_a^H \mathbf{x}_a ^2\}$	$\mathbf{w} = \begin{bmatrix} \mathbf{I} \\ \mathbf{W}_a \end{bmatrix} \mathbf{w}_m$ $\mathbf{W}_a = \mathbf{R}_{aa}^{-1} \mathbf{R}_{am}$	$\mathbf{x}[n] = [\mathbf{x}_m^T[n], \mathbf{x}_a^T[n]]^T$ , $\mathbf{w}_m$ is any conventional weight to steer main sub array to source.
MSNR	$\max_{\mathbf{w}} \frac{\mathbf{w}^H \mathbf{R}_{ss} \mathbf{w}}{\mathbf{w}^H (\mathbf{R}_{ii} + \mathbf{R}_{\eta\eta}) \mathbf{w}}$	$\lambda_{\max} \mathbf{w} =$ $(\mathbf{R}_{ii} + \mathbf{R}_{\eta\eta})^{-1} \mathbf{R}_{ss} \mathbf{w}$	$\mathbf{R}_{xx} = \mathbf{R}_{ss} + \mathbf{R}_{ii} + \mathbf{R}_{\eta\eta}$ i.e. signal + interference, + noise.
SPSN	$\mathbf{w} \in \text{Null}\{\mathbf{R}_{ii}\}$	$\mathbf{w} = P_i^{-1} \mathbf{w}_o$ $P_i^{-1} = \mathbf{I} - \mathbf{U}_i \mathbf{U}_i^\dagger$	$\mathbf{U}_i$ = eigenvectors of $\mathbf{R}_{xx}$ corresponding to $p$ largest eigenvalues.

LCMV: Linear Constraint Minimum Variance

GSC: Generalized Side lobe Canceller

MSC: Multiple Side lobes Canceller

MSNR: Maximum Signal to Noise Ratio

SPSN: Subspace Projection Spatial Nulling

- Adaptive beam forming as LCMV, GSC, MSC, MSNR are suitable for
  - More compact arrays or sub-arrays.
  - Single channel output – array performs as single high gain telescope (like GBT).
  - Candidate for SKA sub-arrays.
- Array nulling: SPSN, modified MSC are suitable for:
  - Large imaging arrays.
  - Output is full array, usable with synthesis correlator.

From the architecture point of view we can have beam formers implemented analogically at the RF level, a multilevel beam formers (Analogue and digital) and all digital beam formers (see figure 2.33, figure 2.34 and figure 2.35).

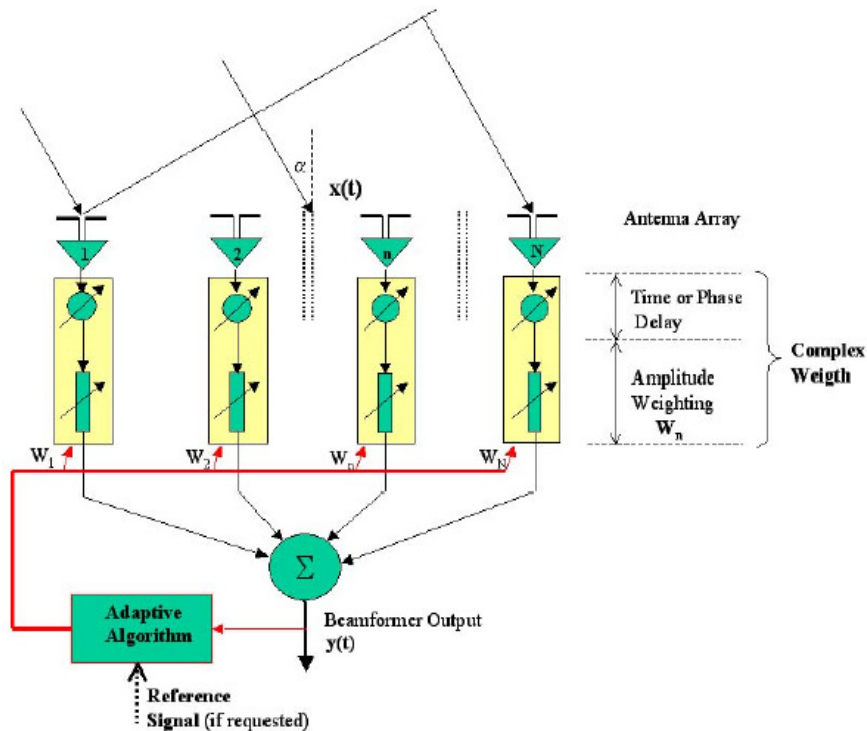


Figure 2.33: Beam former implemented analogically at the RF level

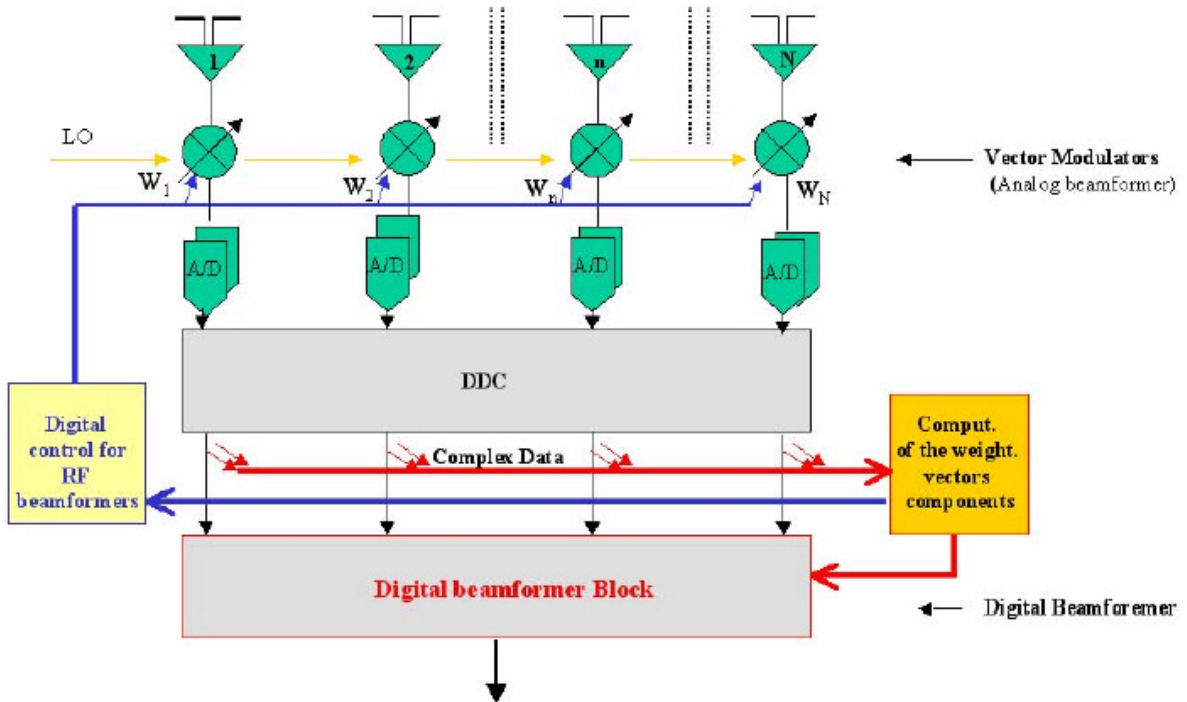


Figure 2.34: Concept of multilevel beamforming (Analogue and digital)

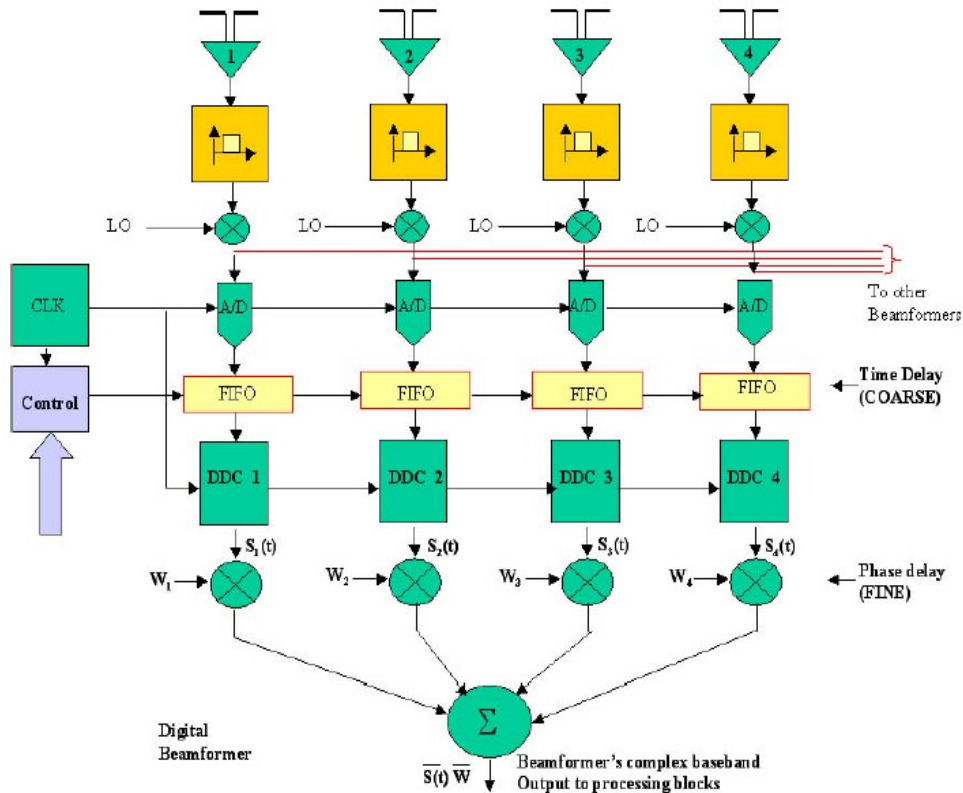
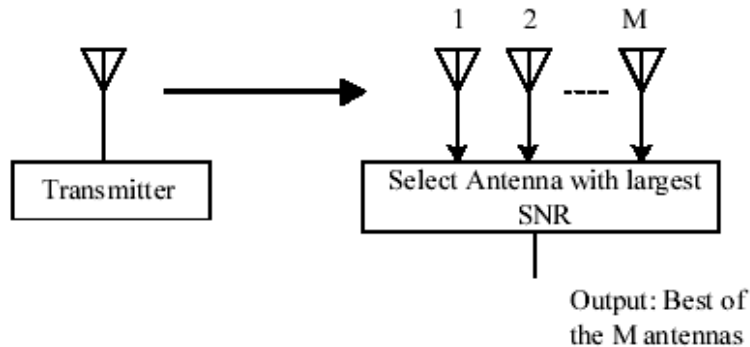


Figure 2.35: Concept of digital beam former implementation

**Diversity:** In addition to phased and adaptive arrays, signals from multiple antennas can be combined to improve performance in fading channels (multipath). The following figures report the block diagrams of three diversity combining techniques. Selection diversity, shown in figure 2.36 is the simplest of these methods.

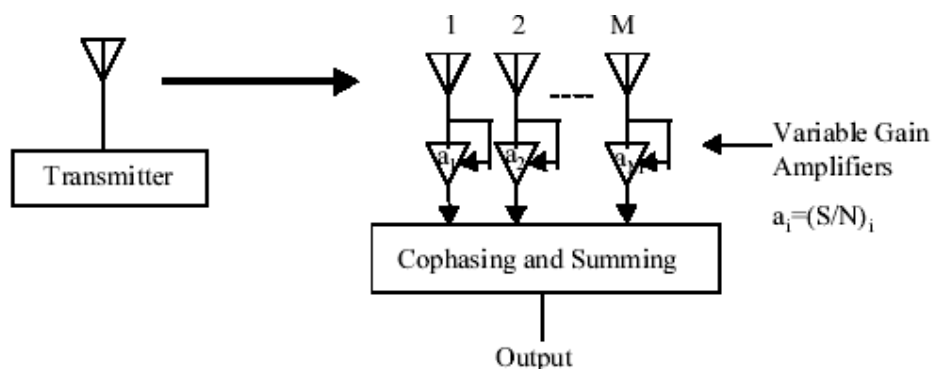


(a)

**Figure 2.36: Selection diversity**

From a collection of  $M$  antennas the branch with the largest signal to noise ratio at any time is selected and connected to the receiver. As one would expect, the larger the value of  $M$  the higher the probability of having a larger signal to noise ratio (SNR) at the output.

Maximal ratio combining takes a better advantage of all the diversity branches in the system. Figure 2.37 shows this configuration where all  $M$  branches are weighted with their respective instantaneous signal voltage to noise ratios. The branches are then co-phased prior to summing in order to ensure that all branches are added in phase for maximum diversity gain. The summed signals are then used as the received signal. Maximal ratio combining has advantages over selection diversity but it is more complicated; proper care has to be taken in order to ensure that signals are co-phased correctly and gain coefficients have to be constantly updated.



(b)

**Figure 2.37: Maximal Ratio Combining**

A variation of maximal ratio combining is equal gain combining (Figure 2.38). In this scheme the gains of the branches are all set to the same value and are not changed thereafter. As with the previous case, the output is a co-phased sum of all the branches [5].

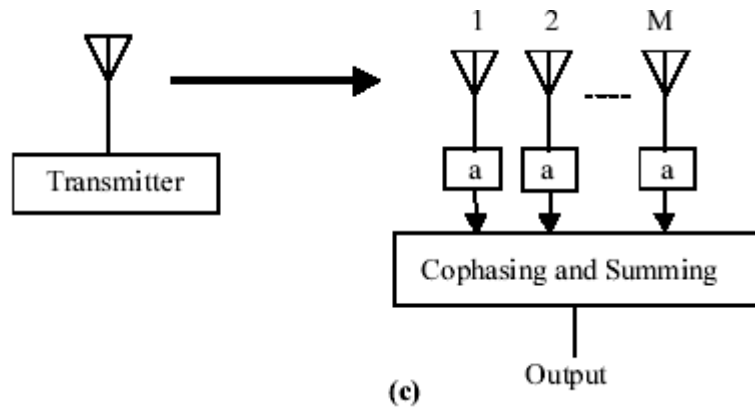


Figure 2.38: Equal Gain Combining

### 2.3.2.1 Efficient Methodology for Beamforming Implementation

#### 2.3.2.1.1 Aspects to be solved

Different beamforming approaches including the problem formulation, the constraints and the optimal solution, were discussed in [1]. We focus here on the implementation methodology of the Beamforming algorithm that can be envisaged for a satellite link. This methodology should take in consideration the following constraints:

- Conceptualization of the mathematical solution,
- Implementation aspects (low complexity, low processing).

The beamformer or the spatial filter has as a function to steer the response of an array of sensors for reception of signal sources in some optimum fashion. When a Least-Squares (LS) solution is considered, the computation of the optimum weights is based on the solution of a system of linear equations known as the deterministic normal equation as:

$$R_x w = v. \tag{1}$$

In (1),  $w$  refers to the vector of the beamformer weights and  $R_x$  denotes the deterministic correlation matrix of the input observation data. The vector  $v$  is the deterministic cross-correlation of the input observation and the ideal signal response. The optimum beamformer weights can then be obtained with inversion of the correlation matrix as:

$$\hat{w} = R_x^{-1} v. \tag{2}$$

From numerical point of view, it is known that the best approach to inverse a matrix is not to do it explicitly. It is instead better to work with the system of linear equations given in (1) and then solve this system using an adequate solution technique.

Traditionally, the implementation of the solution of the system of linear equations given in (1), is done with general purpose DSPs and floating point arithmetic. This type of arithmetic minimizes round-off error making the implementation less sensitive to round-off errors. Such implementations are however limited from a processing power point of view, due to the small number of floating point processing units commonly available per device. A very appealing alternative approach is to use Field-Programmable Gate Arrays (FPGAs) or Application-Specific Integrated Circuits (ASICs) which can provide large amount of parallelism up to hundreds of computational units per device. One complication with such silicon fabrics is that they are typically tailored for fixed-point arithmetic and hence implementation is inherently challenging because of sensitivity to round-off error.

This report presents an efficient methodology that enables the implementation of algorithms involving matrix inversion (such as beamforming) in hardware with fixed point arithmetic.

### 2.3.2.1.2 Beamforming and Matrix Inversion

We consider a narrowband beamformer with  $k$  sensor elements arranged in Uniform Linear Array (ULA). This situation is illustrated in figure 2.39: a signal source  $S_\theta(t)$  is impinging at an angle of incidence  $\theta$  and a  $k$  beamformer weights  $(w_1, w_2, \dots, w_k)$  are used to linearly combine the array data observation samples  $(x_1(n), x_2(n), \dots, x_k(n))$  in order to steer the response of the array for optimum reception. The output of the beamformer is the scalar output  $y(n)$ .

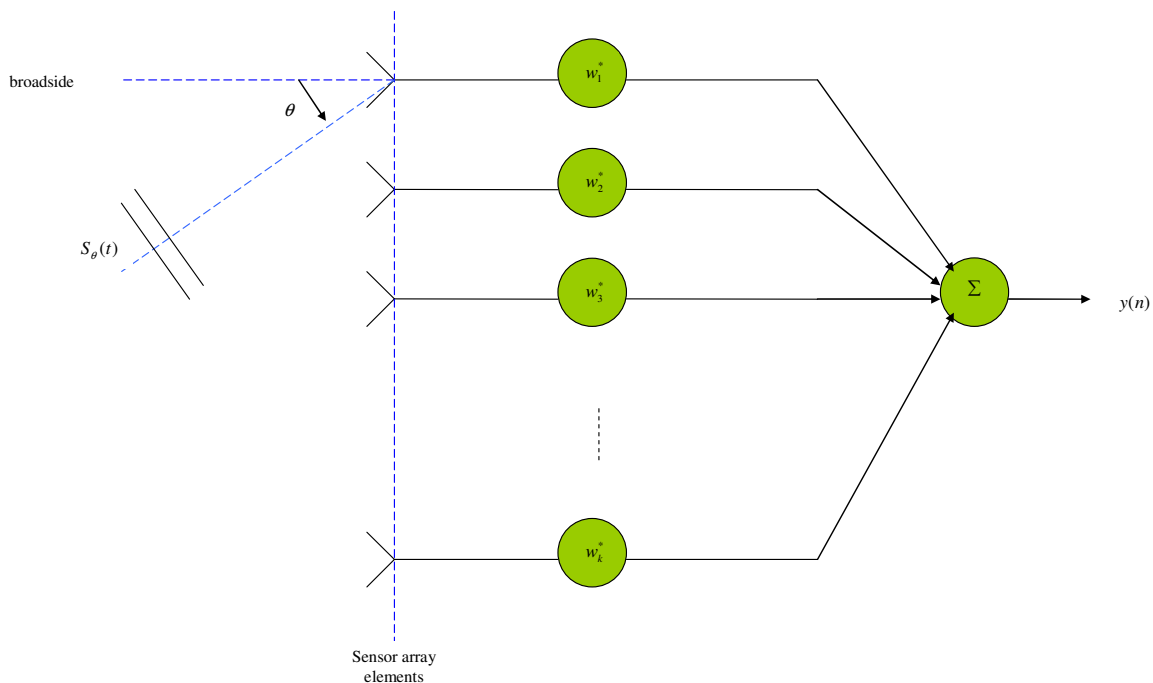


**Figure 2.39: Narrowband Beamforming**

A Generalized Side lobe Canceller (GSC) is a special beamformer architecture that allows the use of unconstrained optimization methods in the determination of the optimum beamformer weights [2]. This architecture is illustrated figure 2.40, where:

- The constant beamformer weights  $W_c$  are designed in a data independent fashion,
- The matrix  $B$  blocks the passing of the input signal of interest in the lower path of the GSC,
- The weights  $W_a$  are determined in an optimum manner according to characteristics of the input data.

With the signal of interest removed, the weights  $W_a$  steer their inputs (containing only interfering signals and noise) to generate a signal that is subtracted from the data-independent path. This effectively cancels, in an optimum manner, the interference from the output of the data independent part.

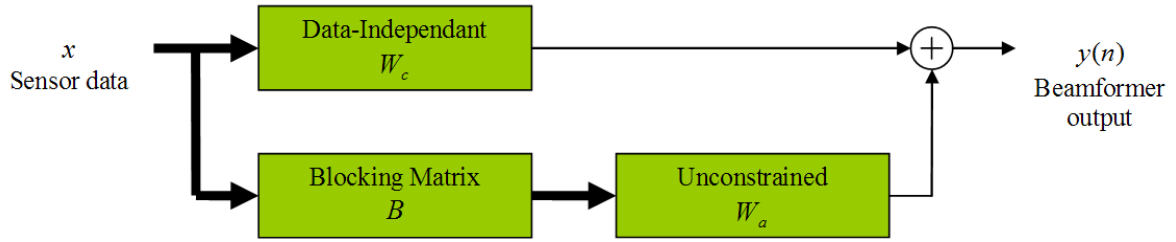


**Figure 2.40: Generalized Side lobe Canceller (GSC)**

In order to find the optimum weights  $W_a$  using the LS criterion, the following deterministic normal equation must be solved:

$$R_x W_a = b. \quad (3)$$

In (3)  $R_x$  is the correlation matrix of the input to the unconstrained section of the GSC, which is  $x_a = xB$  and the vector  $b$  is the cross-correlation of the input  $x_a$  and the ideal response.

An effective technique for solving the deterministic normal equations of (3) is the Recursive Least-Squares (RLS) approximation with Orthogonal-Triangular Decomposition (QRD) of the input data matrix. Mainly, this technique finds the solution without explicit inversion of a matrix and avoids constructing explicitly the correlation matrix, which would reduce the dynamic range requirements of signals involved in the computations.

In order to illustrate the QRD-RLS solution, let  $X_a$  be the input vectors  $x_a$  (assuming a 4-element input vector stacked as columns). Note that this matrix increases in dimension (in number of columns) at every sampling time when a new vector is appended.

$$X_a = \begin{bmatrix} x_{11} & x_{12} & x_{13} & x_{14} \\ x_{21} & x_{22} & x_{23} & x_{24} \\ x_{31} & x_{32} & x_{33} & x_{34} \\ \vdots & \vdots & \vdots & \vdots \end{bmatrix}. \quad (4)$$

For a given sample time  $n$ , with  $n$  columns in the input matrix  $X_a$ , the deterministic correlation matrix of the input is

$$R_{xn} = X_{an}^T X_{an}. \quad (5)$$

Applying the QR decomposition to  $X_{an}$  we obtain

$$R_{xn} = R_n^T Q_n^T Q_n R_n = R_n^T R_n \quad (6)$$

where  $Q_n$  denotes the orthogonal factor of  $X_{an}$  such that  $Q_n^T Q_n = I$  and  $R_n$  is the triangular factor of  $X_{an}$ . Replacing this result in (3) and substituting  $b$  by  $R_n^T Q_n^T d$ , where  $d$  is a column vector with stacked consecutive samples of the desired input signal, we obtain

$$R_n^T R_n w_a = R_n^T Q_n^T d. \quad (7)$$

Assuming that  $R$  is a full rank matrix, then  $R^T$  has an inverse and be eliminated from both sides of (4), which results in

$$R_n w_a = Q_n^T d = p. \quad (8)$$



Equation (8) implies that the LS solution of the deterministic normal equation of (3) can be found for solving for  $w_a$  in the linear system of equations involving  $R_n$ , the triangular factor of the input matrix  $X_a$  and the vector  $p$  resulting from pre-multiplication of the vector  $d$  and the orthogonal factor  $Q_n$ .

The solution of (8) can be obtained recursively. This recursion is justified by the fact that the  $R_n$  factor can be updated recursively every time a new input sample vector is added to the input matrix  $X_{an}$ . In essence, if Givens rotations are used to perform the QR decomposition of  $X_a$ , every time a new input vector is added to  $X_{an}$ , the updated matrix  $R_{n+1}$  factor can be obtained by rotating the elements of the new vector with the previous rows of  $R_n$ .

### 2.3.3 Type of beam forming (pre- vs. post-correlator, if any)

There are different ways to implement the beam forming. The best solution depends from the FPGA selected. From the mathematical point of view most of the operations involved in the correlation process are commutative. From the hardware point of view only some solutions are easily implementable on an FPGA due to the limited number of basic digital operations.

The receiver using the beam forming technique uses a 9 antennas array. Each channel must have the possibility to access to all the 9 signals. The beam forming software needs to independently drive each source of signal for each channel.

Some operations can be merged together or performed in the software.

The mathematical representation of the beam forming coupled with the GPS can be summarized by:

- For each tracking engine channel 9 beam forming units performing the following operations
  - A signal Gain
  - A phase shifter
- Each signal coming out from a beam forming unit enters in a classical tracking engine unit.

The digital hardware implementation of a tracking engine channel coupled with the GPS present some potential problems. The beam forming needs multiplications and increases the resolution of the IF stream. A direct implementation of the mathematical representation will probably need too much hardware resources to fit in a normal FPGA.

Some rearrangement of the mathematical operations can limit the hardware needs; in this chapter 2 solutions are presented.

#### 2.3.3.1 Pre correlation solution with samples buffering

Each signal source stores the samples in a buffer where the exit is controlled by an NCO. This unit is used to control the phase of the signal due to the antenna position on the antennas array.

The exit of each sample buffer enters a gain stage, and then all signals are added together. A scaler limits the resolution of the signal. After scaling the signal enters in the normal GPS correlation channel.

This solution requires a memory for every antenna multiplied by the number of tracking channels. An NCO controls the sample buffer.

The gain multiply the sample by a factor stored in a software accessible register. The register is dimensioned in order to provide the necessary gain (8-10 bits). The multiplier can be implemented using an optimized multiplier where only the possible solutions are implemented (multiplication by -1,-3,1,3).

All the signals are added together. This requires a big adder that can be implemented using a tree of adders in order to reduce the delay path of the signal.

The result of the adder is scaled because the resolution of the signal is too big and without significant improvement.

Figure 2.42 shows the implementation diagram, the scaled signal attacks the classical GPS correlator.

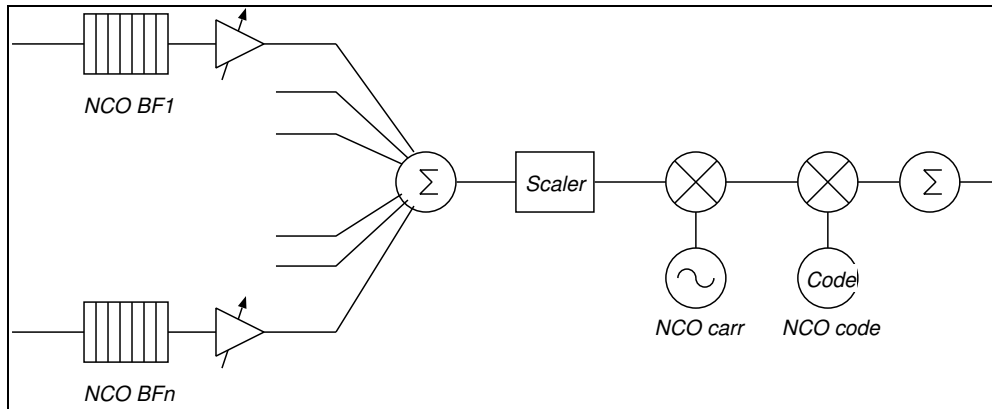


**Figure 2.41: Pre Correlation with samples buffering**

### 2.3.3.2 Pre correlation solution with beam phase controlled by NCO

In this solution the idea is to merge the carrier phase correction due to the Doppler (Doppler remover) with the beam phase correction. The resolution of the NCO controlling the Doppler phase correction should be enough to include even the beam phase correction.

Here the signal of each antenna enters in a mixer where is multiplied by the carrier replica shifted by the Doppler phase plus the beam phase. Then the mixed signal attacks a gain.

All the signals are then added together. The result is scaled just before to enter in the mixer where is multiplied with the C/A replica.

In this case the gain multiplier is bigger because the signal to be treated has a bigger resolution. Even the adder has to handle numbers with a bigger resolution. Figure 2.42 shows the implementation diagram.

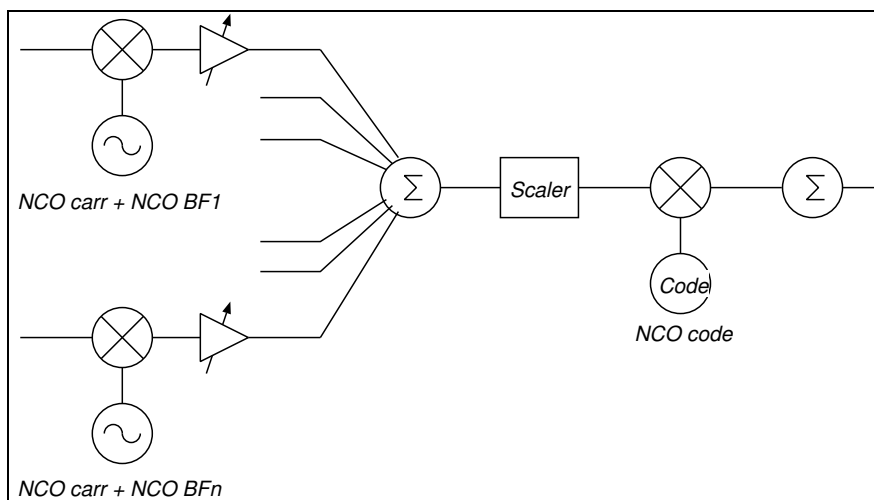


**Figure 2.42: Pre Correlation with phase controlled by NCO**

## 2.3.4 Measurement and navigation engines

### 2.3.4.1 Principe of GRABEL measurements

GNSS positioning process is based on trilateration with a minimum of four pseudorange observations. Doppler on satellite signal carrier can also be used to estimate the receiver velocity. More generally, the so-called navigation filter (typically a Kalman filter) combines pseudoranges, Doppler measurements, noise statistics and a dynamic model to compute a smoothed navigation solution.

GRABEL will enable to track a satellite on various antenna beamforming and polarization configurations (tracking simultaneously direct path and reflected paths on several channels). This would give new measurements with respect to typical GNSS receiver that can be considered as information associated with the antenna environment and orientation.

Outputs of the GRABEL measurement engine are:

- Multipath estimation and mitigation
  - Provide a better estimate of the Time OF Arrival (TOA) of satellite signals thanks to beamforming toward direct path
  - Provide an estimate of multipath errors considering reflected paths impacting a typical omnidirectional antenna (with the ability to detect NLOS situations)
- Angle Of Arrival (AOA) estimation

The role of the enhance localization algorithm is to provide an accurate estimate of position, velocity, time and pose of the user receiver.

AOA observations provide a unique opportunity to estimate pose (antenna axes orientation) that could bring real differentiators for some navigation applications, without the need to use external sensor such as magnetometer or gyroscope. This information is also essential for the GRABEL system, because a variation of the user pose induces a modification of the beam steering toward satellites. This implies to close a loop between outputs of the navigation filter and the beamforming based tracking engines.

### 2.3.4.2 Functional architecture of measurements and navigation engine

Figure 2.43 describes the functional architecture of GRABEL tracking engine and navigation filter processes, showing new functions linked with the AOA determination and the close loop between the navigation filter and the satellite beam forming and tracking channels.

For each of the  $N$  satellite tracking channels, the GRABEL tracking engine determines typical GNSS observations such as signal to noise density ratio ( $C/N_0$ ), pseudoranges ( $\rho$ ), Doppler observation derivate from the estimated carrier frequency ( $f$ ) and carrier phase ( $\phi$ ). Those measurements are estimated from a common correlation process on the signal obtained through a classical Right Hand Circular Polarization (RHCP) omni-directional antenna. This first process corresponds to the coarse TOA and Doppler estimation (the dark grey box on figure 2.43). It applies in a similar way during the acquisition of the signal (searching engine) and during the tracking phase, providing coarse code phase and frequency synchronization to the carrier and code NCO of the beam forming as described in section 2.3.3.

The beam forming process is applied considering the antenna orientation, satellite direction (calculated from demodulated navigation data and previously estimated user position) and potential interferer locations (estimated by the interference rejection module). It consists in a second correlation process, estimating the code phase delay and the frequency offset (with respect to the coarse estimation) that provide the best signal over noise density ratio, while the antenna pattern is forming a beam toward the satellite direction.

A comparison between GNSS observations (with a classical antenna from one side and provided by the beam forming correlation process on the other side) allows evaluating the Line Of Sight (LOS) status of the satellite to user propagation channel. This evaluation can be used by the navigation filter

in order to weight satellite observations or to consider various error models applied on observations while computing user position and velocity.

Finally, the AOA estimation bloc provides an estimate of the offset between the satellite direction and the considered antenna beam, allowing the navigation filter to follow variation onto the antenna orientation.

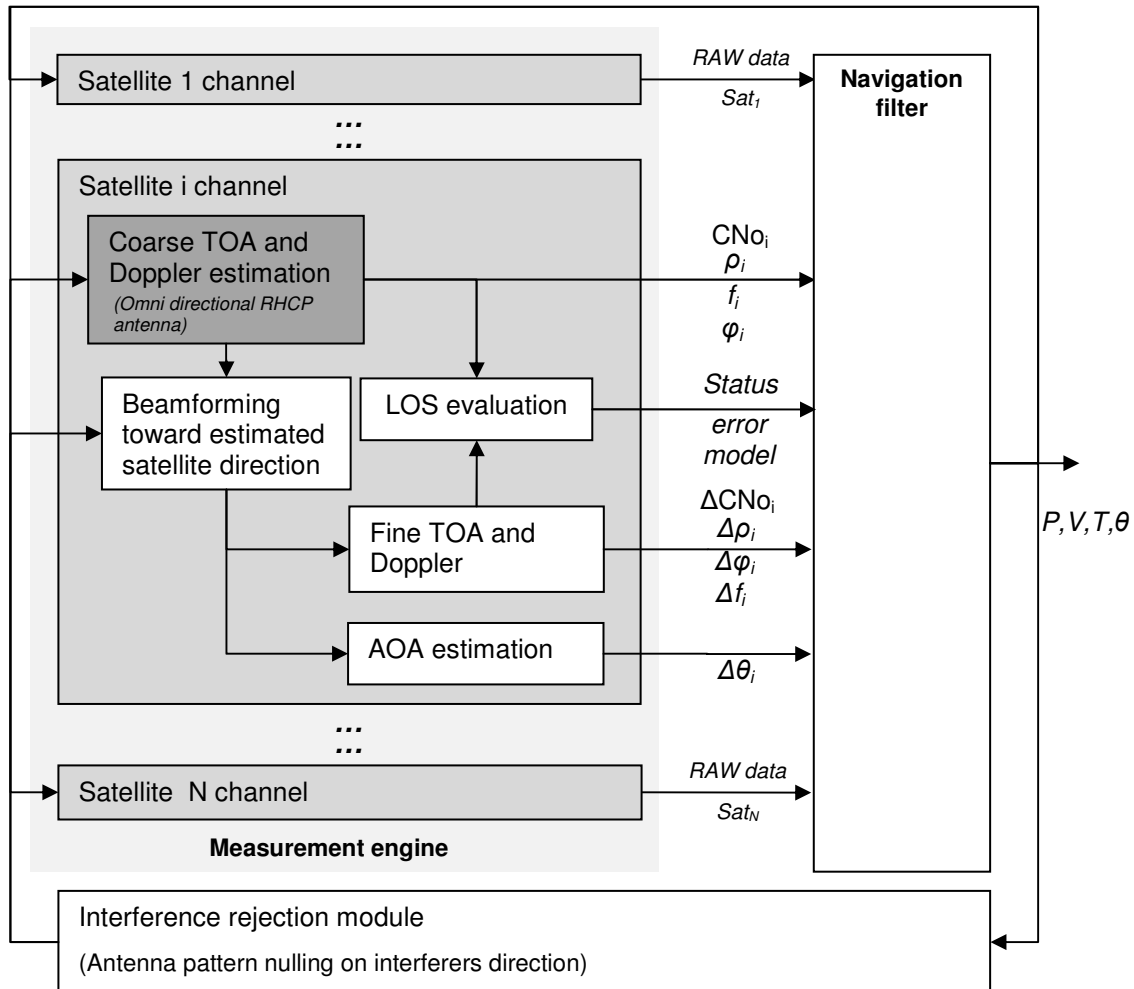


**Figure 2.43: Tracking engine and navigation filter processes**

Another GRABEL specific opportunity should be considered: GRABEL measurements can be used in conjunction with map information, as relative observations on a satellite signal in different directions (beamforming configuration) provide information about the antenna surrounding (existence or obstruction of the direct path is linked with the proximity of buildings...).

The design of the enhanced localization algorithm will be deeply investigated during the WP3.

### 2.3.4.3 Type and number of search and tracking engines

The type and number of correlators needed by GRABEL depends on the beam forming architecture chosen. Frequency domain correlators are very efficient with respect to time domain correlators and will therefore be favoured for GRABEL.

Pre-correlation beam forming (figure 2.41 and figure 2.42) does not require more correlators than a classical receiver does. 16 correlators are therefore sufficient to track the maximum possible number of satellites in view (12 GPS, 2 Galileo, 2 SBAS) with today's GNSS constellations. In order to give some redundancy 20 to 24 tracking channels will possibly be implemented.

If post-correlation beam forming is chosen then the required number of correlators is multiplied by the number of antennas in the beam forming array. 80 to 96 correlators will therefore be required for a 2 x 2 beam forming array. Given the rather large increase of complexity post-correlation beam forming will be implemented only if a significant advantage can be found with respect to pre-correlator beam forming.

Given the planned uses and antenna placements of GRABEL a dedicated search engine is not expected to give a great advantage in signal acquisition. A search engine is therefore not in the base line of GRABEL. If post-correlation beam forming is implemented however the large number of correlators could be easily rearranged to become a parallel correlator search engine with little development effort and hardware (FPGA) cost. In a further development stage a dedicated search engine may be designed. Such search engine will be based on massive correlation, with a performance equivalent to a few 10k correlators. One or (maximum) two search engines are more than sufficient to give fast TTFF even in poor signal conditions and no external aiding.

#### 2.3.4.4 Kind of output and controlling of the receiver

NMEA outputs is the baseline for compatibility with most of existing application software. In parallel (or as a configurable alternative), a proprietary (but open and documented) protocol interface will be used for controlling the receiver and to provide raw data for external simulations and test analysis.

Section 2.3.4.2 defines the main observations that are contained in the so-called GRABEL raw data. Those outputs (serial data transfer) will be the only interfaces of the GRABEL receiver (no screen or other application specific Man Machine Interface).

NMEA output should be compliant with the NMEA 183 (at least version 2.0) standard defined by the National Marine Electronics Association<sup>1</sup>. If necessary (only one physical serial data interface on the board), a proprietary NMEA compliant input message will be used in order to switch to the GRABEL binary protocol.

---

<sup>1</sup> [http://www.nmea.org/content/nmea\\_standards/nmea\\_083\\_v\\_400.asp](http://www.nmea.org/content/nmea_standards/nmea_083_v_400.asp)

## 2.4 Mechanical aspects of GRABEL receiver

One important issue is the antenna system size. Indeed as it is clarified in D1.2 “Use cases and Application Scenarios”, the antenna size, also particularly application dependant, is particularly important. Depending on the application, the GRABEL antenna system could be integrated in or be externalized to the rest of the GNSS receiver. For instance, one GRABEL antenna system would be integrated in a laptop screen holder (figure 2.44). In this case up to 4 SPA-4, with one central element would be integrated. The thickness of the antenna array will target below 4 mm, with bias circuitry and matching network. In terms of operating and storage temperature range, as for shock and vibration resilience, The GRABEL receiver has to cope with classical constraints. For instance the temperature range covers  $-40^{\circ}$  to  $85^{\circ}\text{C}$ . The overall GRABEL antenna size would then be  $30 \times 30 \times 0.5 \text{cm}$  in this case and the weight would not exceed some tens of grams, with PCB stacking and active components and feeding networks.

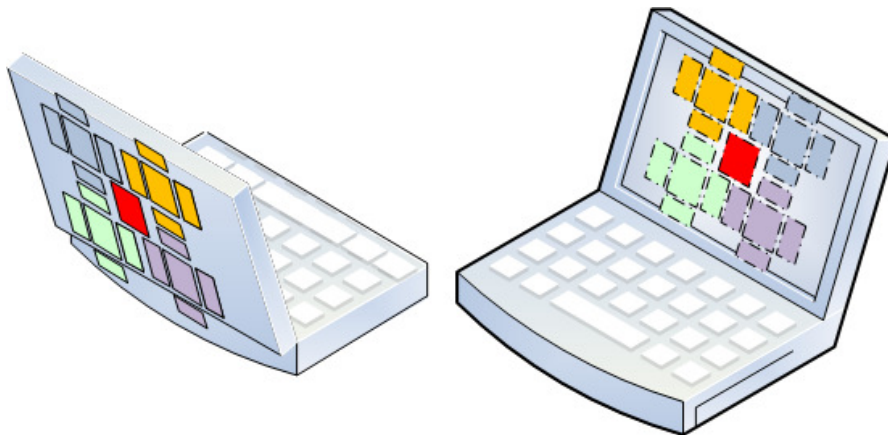


**Figure 2.44: GRABEL antenna system integrated in laptop screen holder**

One other approach is to use remote antenna system as presented on figure 2.45. One concrete application would be roof mounted antenna for emergency vehicle (figure 2.46), which need precise localization regardless the fact that they are moving or not (possibly no inertial unit to Kalman filtering) and WLAN/GSM aided system might not be available in disaster area (earthquake). Such antenna would have a size of 42 cm diameter antenna system with thickness of 5-15mm, depending on the housing to cope with external condition. A radome (see figure 2.46), would be deployed on the roof of the vehicle for instance.

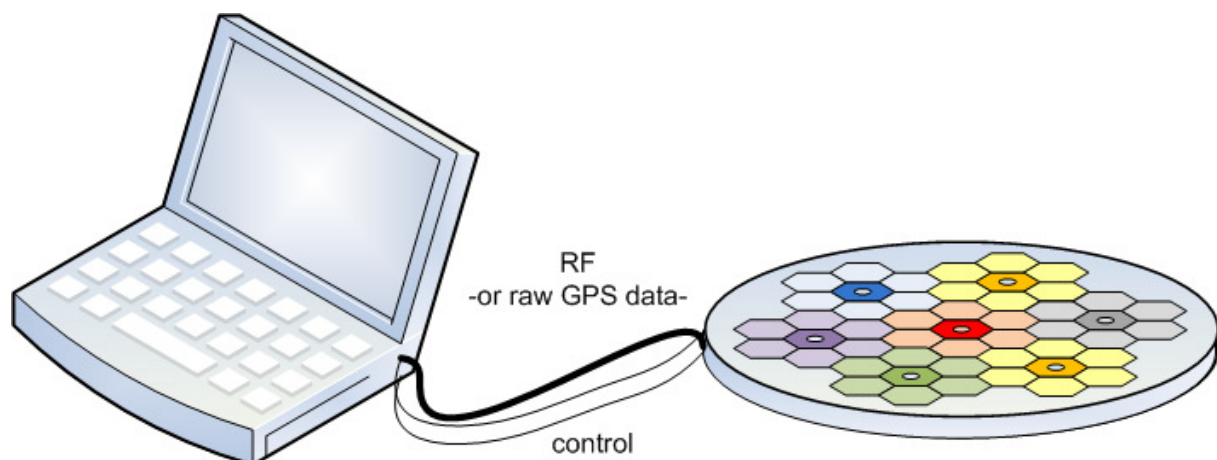


**Figure 2.45: GRABEL antenna system externally connected**

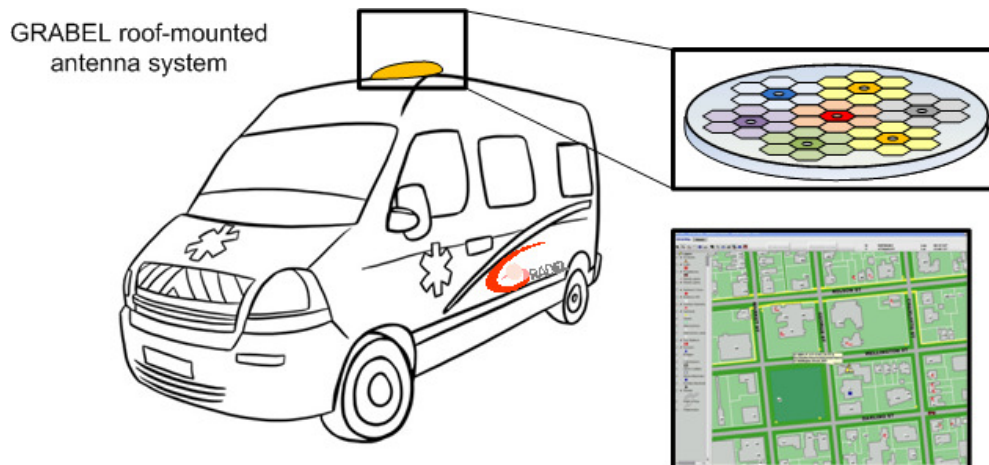


**Figure 2.46: GRABEL roof mounted antenna system for emergency vehicle in urban canyon environment**

---

## 2.5 Application software

In this section, the application software for controlling the GRABEL receiver and for designing and developing the two targeted applications is discussed. Specifically, the application software focuses on a more generic environment in developing location-based services enhanced with components like semantic processing and sensing infrastructure. Such components will be developed and imported to the enhanced application software of the location-based services imported the functionality of the GRABEL receiver. The basic domains of the application software are:

### 2.5.1 Application Software for GRABEL Receiver

The GRABEL receiver uses as default the NMEA183 protocol. This means that virtually any existing navigation software could be used with GRABEL. Anything going from simple "VisualGPS"-style<sup>2</sup> applications to full blown navigation applications sporting any sort of features could be used effectively.

GRABEL however has a few non-standard features that are obviously not supported by standard navigation applications, i.e. support for Galileo and SBAS leads to the possibility to track more than 12 satellites (the NMEA protocol limits the number of satellites to 12), the antenna beam former shall be controlled and the resulting radiation pattern be displayed when requested, while the specific requirements of the two selected applications need to be managed somehow.

Specific application software needs therefore to be developed to take advantage of all GRABEL features. This application software is basically a demonstrator that will typically run on netbooks or small notebook computers. Smaller form factor devices, such as pocket devices, PDAs or embedded systems are not targeted at this time but should not be discarded a priori. Its capabilities shall be summarized as follows:

- Use the output of the GRABEL receiver. This means at least to provide navigation data and capabilities in a form that is suitable to the selected applications. The standard functions, such as mapping and voice synthesis, could also be handled by an existing navigation software to which the input is piped via the GRABEL application software (after conversion to NMEA if necessary) rather than from a /dev/ttyS device.
- Display navigation, direction (heading, also under static conditions) and satellite constellation data. Satellite data shall be displayed for all satellites in view - whether GPS, Galileo or SBAS - and not limited to 12 satellites. This obviously requires that the GRABEL receiver is configured to use the proprietary (but open and documented) protocol rather than its NMEA default.
- Configure all navigation options specific to the selected applications, such as e.g. select the proper user profile (pedestrian, vehicle or static) or configure navigation aids (voice synthesis, language, etc.). Some priority should be given to those functions that are specific to GRABEL and give it value, while representing a differentiator with respect to classical receivers.
- Configure general options (e.g. stay on road) or sanity checks (e.g. disable stay on road if the offset to the indicated position is too big).
- Control, configure and display features of the GRABEL receiver, such as:
  - Select the proprietary protocol to support more features than NMEA allows.
  - Pass to the GRABEL receiver aiding information or DGNSS data (e.g. RTCM104).
  - Configure the antenna beam former, turn beam forming on or off, enable interferer notching.
  - Display antenna-related data, such as direction of the lobes on a satellite-by-satellite basis or direction of the notches for interference rejection.
  - Plot 2D or 3D radiation patterns, again on a satellite-by-satellite basis.

---

<sup>2</sup> <http://www.visualgps.net/>



## 2.5.2 Application Software for Semantic Processing

This software is responsible for design, deploy and reason with the proposed ontologies of the Semantics-based Navigation of Near-Indoor Environments, Specifically, such ontologies are the Near-Indoor Navigation Ontology (NINO) and the User Navigation Ontology (UNO) described in the OWL Web Ontology Language. Ontology describes the concepts and relationships that are important in the applied domain, providing a vocabulary for that domain (user movement characteristics and spatial modeling) as well as a computerized specification of the meaning of terms used in the vocabulary. The two ontologies range from taxonomies and classifications, to fully axiomatized theories. The application software for the design environment for the ontologies is the Protégé software and the reasoning process machine for inferring the best navigation path for the handicapped users is the RacerPro software. Specifically:

- **Protégé<sup>3</sup>** is a free, open-source platform that provides a growing user community with a suite of tools to construct domain models and knowledge-based applications with ontologies. Protégé implements a rich set of knowledge-modeling structures and actions that support the creation, visualization, and manipulation of ontologies in various representation formats. Further, Protégé can be extended by way of a plug-in architecture and a Java-based Application Programming Interface (API) for building knowledge-based tools and applications (link: <http://protege.stanford.edu/doc/dev.html>). The Protégé-OWL editor enables users to build ontologies for the Semantic Web, in particular in the W3C's Web Ontology Language (OWL).
- The **RacerPro<sup>4</sup>** is within the area of description logics. Since description logics provide the foundation of international approaches to standardize ontology languages in the context of the so-called semantic web, RacerPro will be used as the system for managing the semantic web ontologies of NINO and UNO based on OWL. It will be used as the reasoning engine for the ontology editors of Protégé. Finally, RacerPro will be a semantic web information repository with optimized retrieval engine because it can handle large sets of data descriptions (e.g., defined using RDF).
- Application Software for Data Sensing
- Application Software for Designing and Developing

## 2.5.3 Implementation of the Application Software

In order to simplify its deployment, the GRABEL application software shall be portable between different machines and operating systems. At least Linux (as found on most netbooks, several notebooks and on many pocket devices) and Mac OS X or Windows (as found on many notebooks) shall be supported.

In order to simplify portability between operating systems and exchange of code between the consortium's members a common open source development system such as Eclipse and GNU gcc and portable libraries such as Qt (the GUI) and Qwt/QwtPlot3D (graphing, plotting API) should be used. Proprietary non open source software shall be avoided, on limited to the absolute minimum if unavoidable, in the interest of reducing GRABEL development encumbrances and costs.

---

<sup>3</sup> <http://protege.stanford.edu/>

<sup>4</sup> <http://www.racer-systems.com/>

### 3 Conclusions/Summary

A set of general and implementation-specific system requirements were identified within the context of deliverables D1.1 to D1.3. The conceptual/functional decomposition approach followed for the definition of system requirements was mainly concentrated on the following aspects:

- GRABEL Applications Concept
- Reconfigurable antenna features
- Adequate baseband processing.

The tasks carried out in this deliverable involved the system specification of the GRABEL integrated framework. An implementation-oriented approach was followed for the clustering of the GRABEL specified sub-systems and concepts:

- Generic Architecture
- Structure of the antenna system
- Structure of the GNSS receiver
- Architecture of the baseband processor
- Mechanical aspects of the intended receiver
- Application software.

The GNSS receiver specification established in the framework of this deliverable will serve as a basis for the implementation work intended in WP2 and WP3 and later for the demonstrator envisaged as a proof of concept in WP4.

## 4 Reference Documents

**Table 4.1: GRABEL reference documents**

Ref.	Title	Doc.-ID	Version	Date
[RD1]	Definitive Description of Work	DoW_GRABELv12_00	12	21.04.2009
[RD2]	Minutes of KO meeting	Minutes_of_meeting_10_June_2009		10.06.2009

## 5 Bibliography

**Table 5.1: Bibliography**

[Ref.Y]	Complete reference
[1]	D1.1 State of the Art and Technological Roadmaps, 2009.
[2]	Ramon Uribe and Thomas Cesear "Efficient Methodology for Implementation of Matrix Inversion in Fixed-Point Hardware," GSPx 2005, Oct. 24-27, 2005, Santa Clara, CA USA.
[3]	Beamforming Digital Beamforming in Wireless Comm. By John Litva, Artech House EE 233B.
[4]	"Analysis of Adaptive Array Algorithm Performance for Satellite Interference Cancellation in Radio Astronomy" Lisha Li, Brian D. Jeffs, Andrew Poulsen, and Karl Warnick Brigham Young University XXVII URSI General Assembly 2002.
[5]	Kai Dietze, Carl Dietrich, and Warren Stutzman, Vector Multipath Propagation Simulator (VMPS), Draft report, Virginia Tech Antenna Group, April 7, 1999.

- End of document -